Abstract

Cardiac and Mitochondrial Adaptations in Response to Aging and Doxorubicin in Rats Bred for Divergent Aerobic Capacities

by Laura Larion

July, 2012

Director: Dr. Robert Lust

DEPARTMENT OF BIOLOGY

Doxorubicin (DOX) remains as one of the most widely prescribed and effective anticancer agents. A major limitation of the therapeutic effectiveness of the drug is the occurrence of irreversible, progressive, dose-dependent cardiotoxicity. Active aerobic running capacity has been shown to protect against DOX-induced cardiac dysfunction, but little is known of the protective effects of intrinsic non-trained aerobic capacity. We hypothesized that a low aerobic capacity running (LCR) phenotype will be more susceptible for cardiac mitochondrial dysfunction and decreased cardiac performance in response to doxorubicin stress, when compared to the high aerobic running capacity (HCR) animals. To test this hypothesis, cardiac function was assessed in rats specifically selected over 26 generations for their low (LCR) and high (HCR) intrinsic aerobic running capacity. HCR/LCR rats received a single doxorubicin (7.5mg/kg of body weight) intraperitoneal injection and cardiac performance was studied longitudinally through echocardiography. On the tenth day, the animal was sacrificed, cardiac mitochondria were isolated and mitochondrial function was assessed through respirometry studies. Our results indicated that animals with low inherent aerobic capacity were susceptible to doxorubicin insult as evidenced by an adaptive mitochondrial response, while the high aerobic capacity animals appeared to have been physiologically primed and therefore did not exhibit an adaptive compensatory response.

Cardiac and Mitochondrial Adaptations in Response to Aging and Doxorubicin in Rats Bred for Divergent Aerobic Capacities

A Dissertation

Presented To

The Faculty of the Department of Biology

East Carolina University

In Partial Fulfillment

of the Requirements for the Degree

Master of Science

by

Laura Larion

July, 2012

CARDIAC AND MITOCHONDRIAL ADAPTATIONS IN RESPONSE TO AGING AND DOXORUBICIN IN RATS BRED FOR DIVERGENT AEROBIC CAPACITIES

by

Laura Larion

APPROVED BY:

DIRECTOR OF DISSERTATION:_____

Robert M. Lust, PhD

COMMITTEE MEMBER:_____

Barbara J. Muller-Borer, PhD

COMMITTEE MEMBER:_____

Jean-Luc Scemama, PhD

COMMITTEE MEMBER:_____

Terry West, PhD

CHAIR OF THE DEPARTMENT OF BIOLOGY:

_____

Jeff McKinnon, PhD

DEAN OF THE GRADUATE SCHOOL:

_____

Paul J. Gemperline, PhD

Table of Contents

LIST OF TABLES **Page**

LIST OF FIGURES **page**

page

page

CHAPTER I: INTRODUCTION

Prevalence and Cost of Cancer

Prevalence of Cancer

Cancer is one of the greatest public health concerns in the United States (Siegel et al., 2012). According to the American Cancer Society, it is estimated that one in four United States residents will die due to cancer. In the year 2012, approximately 1.5 million new cancer cases and half a million deaths from cancer are projected to occur in the United States. Between genders, the lifetime probability of being diagnosed with an invasive cancer is higher for men (45%) than for women (38%). These statistics demonstrate that cancer is a prevalent cause of mortality and morbidity in the United States, and suggest that current therapies may not be effective at combating this illness.

Cost of Cancer

Cancer accounts for a significant proportion of overall health care costs. The overall annual cost of cancer according to the National Institutes of Health in the United States in 2010 was estimated to be about $260 billion (Scialdone et al., 2012). Direct medical costs accounted for $167.4 billion and lost productivity accounted for $119.2 billion (NHLBI, 2010). One study calculated that an individual's treatment cost for the initial year after diagnosis can vary from $18,052 for a less invasive cancer to $42,401 for more advanced stages (Lang et al., 2009). The financial impact of cancer is not only costly for society, but also to the individual, as the direct and indirect costs of cancer to a patient can be devastating. Therefore, cancer's burden on the nation is expensive (Ershler, 2003; Brown et al., 2001; Chang et al., 2004).

Cost-effectiveness Analysis of Chemotherapy

Due to its extensive incidence and high cost, improvement in the prevention, early detection and treatment of cancer is a major priority of medical research (Chang et al., 2004). Current cancer treatment options include surgical intervention, radiation and anti-tumor chemotherapy. Anticancer therapy aims to maximize the beneficial antitumor results while minimizing unwanted side effects and cost of treatment, to achieve the best outcome for the patient. Treatment evaluations of the cost of cancer care incorporate a large number of variables, making patient benefit-versus-cost management decisions difficult for oncologists and patients (Keefe et al., 2012). Despite their relative antitumor efficacy, a common patient survival value/benefit-versus-cost adjustment to chemotherapy treatment is attributed to the non-selective cytotoxicity side effects, such as myelosupression, nausea and vomiting, mouth ulcers and alopecia (Kizek et al., 2012). Serious adverse side effects force patients who may otherwise benefit from continued administration of a drug to withdraw from chemotherapy and switch to an alternative agent, which may be less effective (Swain et al., 2003).

Doxorubicin-induced Cardiotoxicity

Doxorubicin chemotherapy treatment

Toxic side effect limitations to chemotherapy is especially true for the anticancer agent doxorubicin (DOX, adriamycin), in this case due to its notorious cardiotoxic side effects (Greish, et al., 2004). Since the drug's discovery in 1969 from *Steptomyces peucetius,* a species of actinobacteria, it has been one of the most effective and prescribed antitumor clinical agents due to its wide spectrum of cytotoxicity (Arcamone et al., 1997;Simunek et al.,

2009; Singal et al., 1997; Swain et al., 2003). The chemical structure consists of a tetracycline moiety containing a quinone and a conjugated amino sugar residue (Fig. 1) (Berthiaume et al., 2007). Doxorubicin is part of a group of anticancer drugs known as anthracyclines (ANTs) which are well established as successful antineoplastic antibiotics for various hemopoietic and solid malignancies, such as breast and esophageal carcinomas; osteosarcoma, Kaposi's sarcoma and soft-tissue sarcomas; and Hodgkin's and non-Hodgkin's lymphomas (Bristow et al. , 1978; Hortobagyi et al, 1997; Singal et al., 1998).

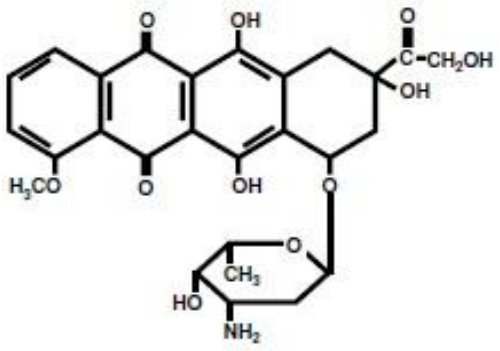

Figure 1. The structure of Doxorubucin (Berthiaume et al., 2007)

However, due to the drug's small molecular size (543 Da), it lacks specificity to cancer cells and can be distributed to rapidly dividing cells, such as bone marrow and intestinal epithelial cells (acute toxicity) or more stable tissues, such as cardiac and hepatic tissues (chronic toxicity) (Greish et. al, 2004). Doxorubicin is known to accumulate preferentially in the heart creating a cardiotoxicity that causes organ dysfunction. This limits the administration of the drug to a cumulative dose exceeding ~500mg/m^2 body surface area

(Singal et al, 1997). Thus, those with prior cardiac conditions are contraindicated from this medication, and precautions must be taken as the risk of cardiomyopathy is expected to increase in terms of severity and frequency in a linear dose-dependent manner (De Los Santos et al., 2000; Wondergem et al., 1991).

Cardiotoxicity

Four types of anthracycline-induced cardiotoxicity have been recognized (Ferrans et al., 1997; Hrdina et al., 2000; Jones et al., 2006; Shan et al., 1996; Simunek et al. , 2009; Wouters et al., 2005). First, "acute" cardiotoxicity occurs immediately after administration and typically causes vasodilation, hypotension, and transient changes in cardiac rhythm (Ferrans et al., 1997). These disturbances usually reverted to normal and were mainly seen in adults (Hale et al., 1994). Second, "subchronic" or "subactute" cardiotoxicity manifests 1-3 days after treatment as a pericarditis-myocarditis syndrome. This cardiotoxicity is uncommon and was particularly evident in the early trials of ANT treatment using very high doses in a short amount of time (Hale et al., 1994; Simunek et al., 2009). "Early chronic" is the third type of cardiotoxicity that develops weeks or months after the administration of the chemotherapy. It is characterized by dilated cardiomyopathy, left ventricular dysfunction and congestive heart failure (CHF) within a year after the completion of ANT therapy (Ferrans et al., 1997; Shan et al., 1996). Finally, "delayed" or "late-onset chronic" cardiotoxicity manifests years to decades after the completion of treatment, after a prolonged asymptomatic period. This latent toxicity was recognized at the start of the 1990s among adults who have survived pediatric cancers (Shan et al., 1996; Simunek et al., 2009). Patients with cardiomyopathy due to DOX-induced toxicity have an especially poor

prognosis, as their survival chances are worse than patients with ischemic cardiomyopathy (Felker et al., 2000). As the number of long-term cancer survivors continues to increase, chronic cardiotoxicity remains a clinically significant problem as the cardiac damage acquired after DOX-infusion is irreversible and progressively worsens.

Several studies have attempted to explain the predilection of heart tissue to DOX-toxicity. To begin with, the drug seems to be retained in cardiomyocytes more than in other cell types (Johnson et al., 1986). The exact pathogenesis of DOX-induced cardiotoxicity remains unclear although it is hypothesized that the drug exerts its antineoplastic and cardiotoxic action by distinct mechanisms: the anticancer response has been associated with lipid peroxidation, DNA intercalation, and inhibition of protein synthesis enzymes such as topoisomerase II (Arai et al., 2000; Arola et al., 2000; Billingham et al., 1978; Doroshow et al., 1986; Greish et al., 2004; Muller et al, 1998; Myers et al., 1977; Singal et al., 1998; Wang et al, 2004). All of these effects result in cell cycle arrest that culminates in pro-apototic machinery leading to the death of cancer cells and tumor growth arrest (Pereira et al., 2011). There is increasing evidence that oxidative and pro-apoptotic stressors are the primary causal mechanisms responsible for the cardiotoxic activity (Lai et al, 2011; Ludke et al., 2011; Tokarska-Schlattner et al., 2006). Evidence suggests that the chemical structure of doxorubicin is prone to the generation of free radicals, leading to an increase in toxic reactive oxygen species (ROS) produced by the mitochondria, which trigger DNA damage and induces intrinsic mitochondria-dependent apoptotic pathways in cardiomyocytes (Koka et al., 2010; Mokni et al., 2012 Rajagopalan et al., 1988). Interestingly, this oxidative stress pathway has been found to be distinct from DOX-induced apoptosis induced in tumor cells

(Wang et al., 2004). This suggests that the principal cause of cardiac damage induced by the drug is through oxidative stress interaction with the myocardial mitochondria.

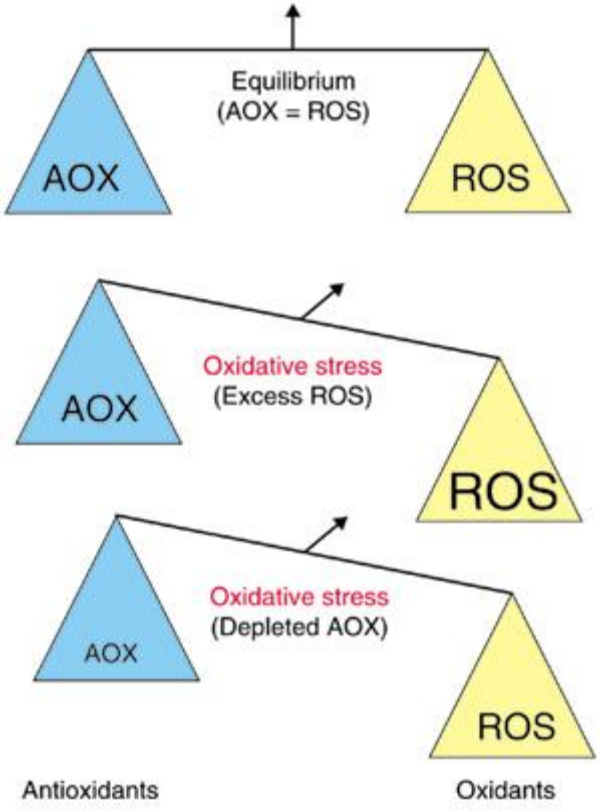

Figure 2. Equilibrium and loss of balance scenarios between oxidants (ROS) and antioxidants (AOX). Under normal conditions, there are sufficient antioxidants to overcome the ROS. A state of oxidative stress occurs when either ROS production is excessive or antioxidants are inadequate (Scandalios, 2002).

Mitochondria and the Oxidative Stress Hypothesis

Oxidative stress is the accumulation of reactive oxidative species beyond the capacity of antioxidants that damage important components inside the cell (Fig. 2) (Ago et al., 2010; Alexeyev, 2009). Oxidative stress is caused by free radicals or hydrogen peroxide derivatives

containing a free unpaired electron on its outer electron shell, thereby making them highly reactive and unstable (Cecarini et al, 2007). These molecules mutagenize proteins, lipids or nucleic acids and render them incapable of properly functioning. More specifically, oxidative stress is the difference between the concentration of oxidants necessary and beneficial for a cell in order for it to regulate physiological processes, and the uncontrolled oxidation caused by unregulated ROS production (Hole et al., 2011). Normally, an oxidative burst in conjunction with oxidative leakage from cellular respiration as well as with environmental factors causes the production of superoxide (O_2). Superoxide dismutase (SOD) will convert the superoxide ions into hydrogen peroxide (H_2O_2), which will then be converted further into water and molecular oxygen by the enzyme catalase, reduced into water by glutathione peroxidase, or generate highly toxic hydroxyl radicals (OH) through catalytic transition metals, especially iron (Fe) (Fig. 3) (Simunek et al., 2009; Zhou and Kang, 2000). However, in situations of increased superoxide concentration, hydroxyl (OH) free radicals may form that are extremely reactive and cause protein and lipid peroxidation and DNA damage. The accumulation of cellular injury results in cell death (Ferrari, 1996). The primary generators of ROS in cells and tissues are mitochondria.

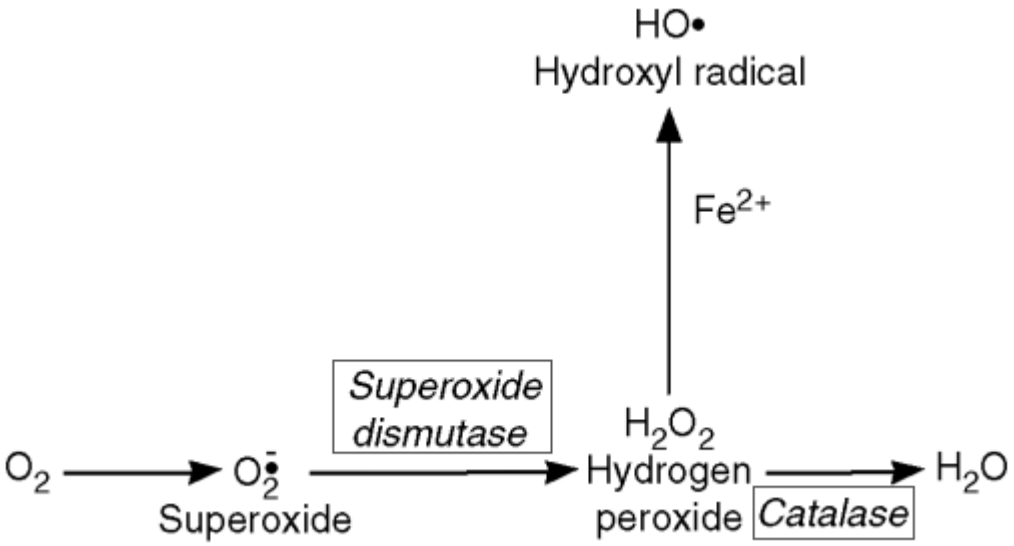

Figure 3. Generation of ROS (modified from Shah, 2004).

To meet the heart's energetic demands, cardiomyocytes contain a very high mitochondrial content (30-40% of the cellular volume) relative to other organs (Yan et al., 2008). The primary function of myocardial mitochondria is to generate ATP to support rhythmic contraction of the myocardium (Williamson, 1979). Through oxidative phosphorylation, the mitochondrial electron transport chains (ETCs) consume oxygen to convert into cellular energy in the form of ATP, which fuel cardiac contractile work (Stanley et al, 2004). Although there are numerous endogenous producers of ROS, mitochondria continue to be significant sources of oxidant production. Mitochondria are the largest source of intracellular oxidant production in cardiomyocytes and approximately 1-2% of the electrons in the ETC leak to form superoxide anion, which is further converted into other ROS species (Anderson et al., 2011; Yan et al., 2008). Unfortunately, it is theorized that cardiac tissue has a less developed antioxidant defense system as catalase has not been

detected in the mitochondria except in rat myocardial cells (Nediani et al., 2011; Radi et al., 1991). Since nearly 90% of ROS in cardiomyocytes can be traced back to the mitochondria, these organelles are a major source of ROS production and must maintain ROS at appropriate concentrations to prevent excess oxidation that, in turn, leads to further mitochondrial damage (Ago et al., 2010Balaban et al., 2005; Nicolson et al., 2008).

In addition to being sources of oxidants, cardiac mitochondria are also uniquely susceptible to oxidative stress damage via doxorubicin (Johnson et al, 1986). Deleterious effects on mitochondrial bioenergetics are thought to be the primary targets of the drug's cardiotoxicity (Chandran et al., 2009; Yen et al., 1996). After administration of doxorubicin in laboratory animals and humans, the generation of ROS and lipid peroxidation products increases while tissue antioxidant levels decrease (Conklin, 2005). Moreover, the amount of DOX-induced oxidants rises up to 10 times greater in the heart than it is in other tissues such as the liver, kidney and spleen (Conklin, 2005). The ability of doxorubicin to generate high levels of oxidative stress is due to the quinone moiety in its chemical structure. The drug has a high affinity for cardiolipin, a relatively cardiospecific negatively charged phospholipid that is found in the inner membrane of the mitochondria (Simunek et al., 2009; Wallace, 2003). Once inside the mitochondria, it can be reduced by the ETC into an unstable semiquinone. This radical intermediate is then oxidized, transferring an electron to oxygen to produce superoxide anion radicals that subsequently generate highly reactive hydrogen peroxide and other ROS (Esmat et al., 2012; Gilliam et al., 2012). This redox cycling behavior of doxorubicin initiates a cascade of free radicals which oxidize DNA bases, lipids, and proteins leading to a loss of cell integrity, enzyme function, and genomic stability (Esmat et al., 2012;

Trachtenberg et al., 2011). As these unique modifications in the cardiac mitochondrial electron transport system can lead to cell death and ultimately organ damage, it is considered the primary mechanism underlying DOX-induced cardiotoxicity.

Moreover, as the heart is a post-mitotic organ with low cardiomyocyte turnover rate (approximately 1% per year at age 20, declining to 0.4% per year at age 75), the oxidative damage will accumulate with time and the remaining undamaged cardiomyocytes cannot reconstitute the lost cardiac tissue, causing the heart to deteriorate functionally with time (Murry et al., 2009). Therefore, due to the vital role that mitochondria play in cellular metabolism, dysfunction of this organelle as a result of doxorubicin-induced oxidative stress can have dire consequences. Dox-induced ROS may damage mitochondrial functions, such as oxidative phosphorylation, depressing myocardial ATP necessary for the energetic demands of the heart (Berthiaume et al., 2007). In order to protect the heart's energy production machinery to allow for normal cardiac contractile performance, cardiac oxidants must be kept in balance. Expanding our understanding of how to reduce reactive oxygen species overload will assist in preserving the integrity of the mitochondria in the face of oxidative stress and prevent fatal organ damage through cardiac toxicity.

Prevention of DOX-Induced Cardiotoxicity

Aerobic Capacity

As there is no effective treatment presently available for Dox-induced cardiotoxicity, prevention remains the best therapeutic. The aim of prevention is not only to prevent the toxicity, but also to increase the antitumor efficacy (Pereria et al., 2011). To circumvent the adverse side effects of doxorubicin, aerobic capacity and exercise have been suggested as

one of the few countermeasures to alleviate acute and chronic cardiotoxicity (Khakoo et al., 2011). Maximal aerobic capacity is represented by the measure of maximal oxygen consumption (VO_{2max}) typically by maximal treadmill running. The higher the $VO_{2max,}$ the greater the cardiovascular system has the ability to transport oxygen to the exercising muscles (Fitts et al., 1994). This is a standard tool that assesses the fitness of an individual and diverges with other cardiovascular dysfunction risk factors, such as cardiac energy substrate utilization, expression of key mitochondrial proteins, oxygen transport, and susceptibility to cardiac arrhythmias (Palpant et al., 2009) Studies have shown that exercise capacity is a strong predictor of early morbidity and mortality, and a clinical retrospective study demonstrated that low exercise capacity is a stronger predictor an increased risk of death than other established risk factors, such as hypertension, diabetes, or smoking (Koch et al., 2011; Myers et al., 2002). Thus, aerobic capacity is implicated in both an immediate functional performance perspective and from a prospective survival outlook (Rognmo et al., 2004).

Exercise preconditioning attenuates DOX-induced oxidative stress

Aerobic exercise capacity can be divided into (i) adaptational (as a response to active exercise training) or (ii) intrinsic (untrained) phenotypic profiles (Koch et al., 2008). Studies have shown that the first type of aerobic exercise, which includes walking, running, treadmill, cycling and calisthenics, causes weight loss, decreased insulin resistance, increased aerobic capacity, decreased lipids, decreased systolic blood pressure and decreased inflammation (C-reactive protein) (Moinuddin et al., 2012). The benefits of aerobic exercise training are well established as regular exercise has been shown to reduce the risk of heart

disease, control hypertension and protect the heart against oxidative stress and apoptosis (Wonders et al., 2008). Moreover, exercise has been shown to reduce arrhythmia, decrease myocardial stunning, and improve vascular reactivity in hearts exposed to ischemia-reperfusion (Frasier et al., 2011). In regards to doxorubicin-induced toxicity, there are various exercise training regimens - acute vs. chronic (repeated) - that have shown that exercise preserved cardiac function in mice receiving the drug (Jones et al., 2010). More specifically, exercise alleviates doxorubicin toxicity by improving antioxidant status, attenuating apoptotic pathways, and preserving contractile function expression. It is theorized that exercise training induces increases in catalase and glutathione peroxidase activities which are beneficial under elevated ROS conditions, such as when induced by DOX as the drug has been shown to induce additional ROS production in mitochondria and increase oxygen consumption by a factor of six (Ascensao et al., 2005; Martins et al., 2012). Thus, exercise may confer a protective preconditioning effect against DOX-induced ROS generation.

Intrinsic aerobic capacity

There is plenty of evidence indicating that regular physical activity can aid in the prevention and treatment of a wide assortment of cardiovascular ailments and is a significant, modifiable behavioral risk factor (Armstrong et al., 2006). However, not everyone is physically able to exercise, and in some cases, hospitalization for immune complications associated with either the cancer or its treatment may preclude exercise. In either case, the role of the latent capacity for aerobic exercise in the overall response is not clear, but certainly important. However, much less is known about how intrinsic aerobic capacity,

independent from active exercise, plays a role in predicting cardiovascular fitness. Twin and family studies have supported the heritability of intrinsic aerobic capacity as both the ability to perform and the propensity to engage in exercise (Waters et al., 2008). The HERITAGE Family investigated the genetic contribution to the untrained fitness level as well the potential of training-induced improvements (Blouchard, 2012). They explored the adaptational response to exercise by engaging 742 healthy but sedentary subjects in a highly standardized, well-controlled endurance-training protocol for 20 weeks and recorded the VO_{2max} response. They observed that the varied response that some individuals were highly trainable while others had little or no benefit to training. The heritability was determined to be 47% for the VO_{2max} response, with a maternal transmission of 28%. Also, there was a reported 2.5 times more variance between families than within families. This raised the possibility that mitochondrial DNA is involved in heterogeneous response to training and that there is a significant genetic basis to exercise (Bouchard et al., 1999).

HCR/LCR animal model

To further study the genetic contribution of aerobic capacity, Koch and Britton developed two strains of rats with marked differences in intrinsic aerobic exercise capacity phenotypes (Koch et al., 2001). This was accomplished by two-way artificial selective breeding of rats that exhibited either high capacity (HCR) or low capacity (LCR) endurance treadmill running capacity. In 1996, the research group initiated a breeding project consisting of 96 male and 96 female rats using the genetically heterogeneous rat population from N:NIH (National Institutes of Health) stock as the founder population. At 11 weeks of age, running capacity was assessed by using an incremental velocity treadmill running

protocol. Intentional crossbreeding of 13 lowest- and 13 highest-capacity rats of each sex were selected and randomly paired for mating. Genetic variance among the population was maximized by not selecting among brothers and sisters. After 11 generations of selection, the LCR and HCR rats differed by 347% in aerobic running capacity. In 2007, 21 generations of selection had been performed and there was a 461% divergence in running capacity. The difference in VO_{2max} was due largely as a consequence of changes in the capacity to deliver oxygen to the exercising muscle; HCR rats had a greater maximal cardiac output (Koch et al., 2008). This divergent animal model yields rats that can be studied without potentially confounding additional environmental adaptations that occur with exercise training (Lessard et al., 2009).

Current results suggest that HCR/LCR rats can serve as genetic models that contrast for disease risks and indirectly support a mechanistic role for oxygen metabolism (Koch et al., 2008). Thus far, many studies have observed divergent characteristics between these model organisms. LCR rats have accumulated cardiovascular risk factors, such as a large gain in visceral adiposity, hypertension, dyslipidemia, impaired glucose tolerance, endothelial dysfunction, hyperglycemia, hypertriglyceridemia, insulin resistance and elevated plasma free fatty acids (Koch et al., 2011; Wisloff et al., 2005). In addition, LCR rats have decreased stroke volume, reduced systolic and diastolic cardiac function, as well as impaired oxygen supply extraction ratio and tissue diffusion capacity in skeletal muscle as compared to HCR rats (Hoydal et al., 2007). Moreover, LCR rats expressed decreased levels of proteins involved in mitochondrial function in skeletal muscle, supporting the notion that impaired regulation of oxidative pathways in mitochondria may be a linkage between aerobic capacity and

cardiovascular disease (Wisloff et al., 2005). In summary, LCR rats score high on disease risks associated to the metabolic syndrome, which is defined as collection of symptoms that may predispose for cardiovascular disease, and HCR rats score high for health factors related to maximal oxygen consumption (Koch et al., 2008). LCR rats also respond more negatively to environmental health risks, such as high fat diets (Noland et al., 2007). Therefore, it would be worthwhile to examine how this aerobic rat models respond differentially to doxorubicin-induced cardiotoxicity.

Goal of Current Study

Based on previous studies of diverging susceptibilities for cardiovascular risk factors between LCR and HCR rats, we hypothesized that indexes of cardiac function after doxorubicin administration (stressor) would co-segregate with intrinsic aerobic capacity. We hypothesize that the rats will exhibit differential responsiveness to doxorubicin-induced cardiotoxicity.

We hypothesize that an attenuated aerobic capacity as found in LCR rats has a genetic profile that is deficient in their antioxidant defenses and mitochondrial functions. Therefore, with a diminished ability to metabolize and detoxify oxygen, they are left more susceptible to the oxidant burden of doxorubicin.

Therefore, the aim of this thesis was to study the influence of intrinsic aerobic exercise capacity on metabolic and cardiac adaptive responses to doxorubicin-induced toxicity, and tests the overall hypothesis that the low aerobic endurance running capacity (LCR) phenotype will show altered metabolic and cardiac responses to doxorubicin when

compared to the high aerobic endurance running capacity (HCR) phenotype. Moreover, we expect that the HCR phenotype confers cardioprotection against doxorubicin-induced cardiotoxicity as compared to the LCR phenotype.

CHAPTER II: METHODS

Animal Care

Female HCR/LCR rats were obtained from Drs. Lauren Koch and Steven Britton at the University of Michigan (aged approximately 25 months) and obtained from *generation 26*. The creation of the HCR/LCR rat model has been previously described in detail (Britton, 2005; Koch et al., 2001; Koch et al., 2008). All animals were housed 2 per cage in a temperature-controlled 12/12-hour light/dark cycle facility, where standard rat chow and water were provided *ad libitum*. Rats were randomly assigned into four groups: LCR injected with saline, (LCR + SAL) (*n*=6), LCR injected with DOX (LCR + DOX) (*n*=9), HCR injected with saline (HCR + SAL) (*n*=3) and HCR injected with DOX (HCR+DOX) (*n*=5). The number of rats in the LCR + DOX and HCR + DOX groups was greater to accommodate the potential mortality following DOX. All protocols were approved by the Brody School of Medicine at East Carolina University Institutional Animal Care and Use Committee and were in compliance with Animal Welfare Act guidelines.

Doxorubicin Administration

The LCR + DOX and HCR + DOX groups received a single intraperitoneal DOX injection (7.5mg/kg of body weight), while the control groups received an injection of 0.9% sterile saline at equivalent volumes.

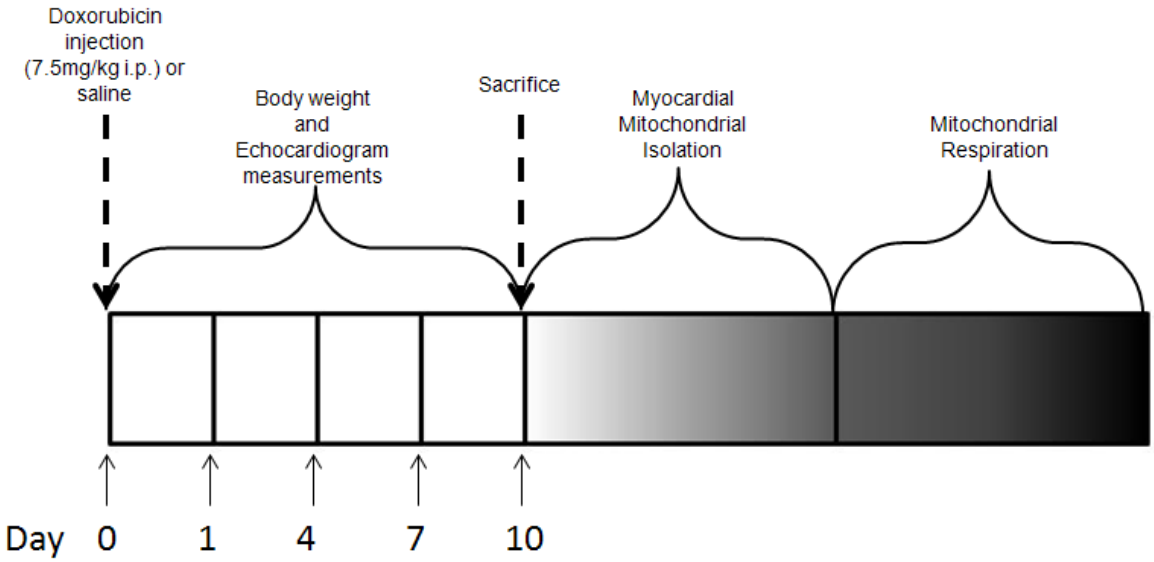

Figure 4: Schematic representation of the experimental schedule used for assessing the Doxorubicin-induced cardiotoxicity in the rat. Solid arrows denote body weight measurements and ultrasounds. i.p., intraperitoneal.

Assessment of Cardiac Function

Transthoracic echocardiography was conducted on sedated rats using a commercially available echocardiographic system (Vevo 2100, Visual Sonics Inc., Toronto, Ontario, Canada) with a 13-24 MHz linear array transducer (MS250). Echocardiogram and body weight measurements were made prior to injection (baseline) and 1, 4, 7 and 10 days post-injection (fig.1). Rats were anesthetized by isoflurane (2-2.5%) delivered through a nose cone and the echocardiography was completed within 15 minutes after the administration of the sedative. The hair on the thoracic area was removed by applying a depilatory. Ultrasound transonic blue gel was placed on the thorax to optimize visibility. Two-dimensional images of the left ventricle were obtained in the parasternal long-axis and short-axis views. B and M-mode images were obtained at the midventricular level in both views, from which internal

dimensions of the left ventricle were obtained at end diastole and end systole (Figures 5 and 6). All images were analyzed using Vevo 2100 1.3.0 software (Visual Sonics Inc.).

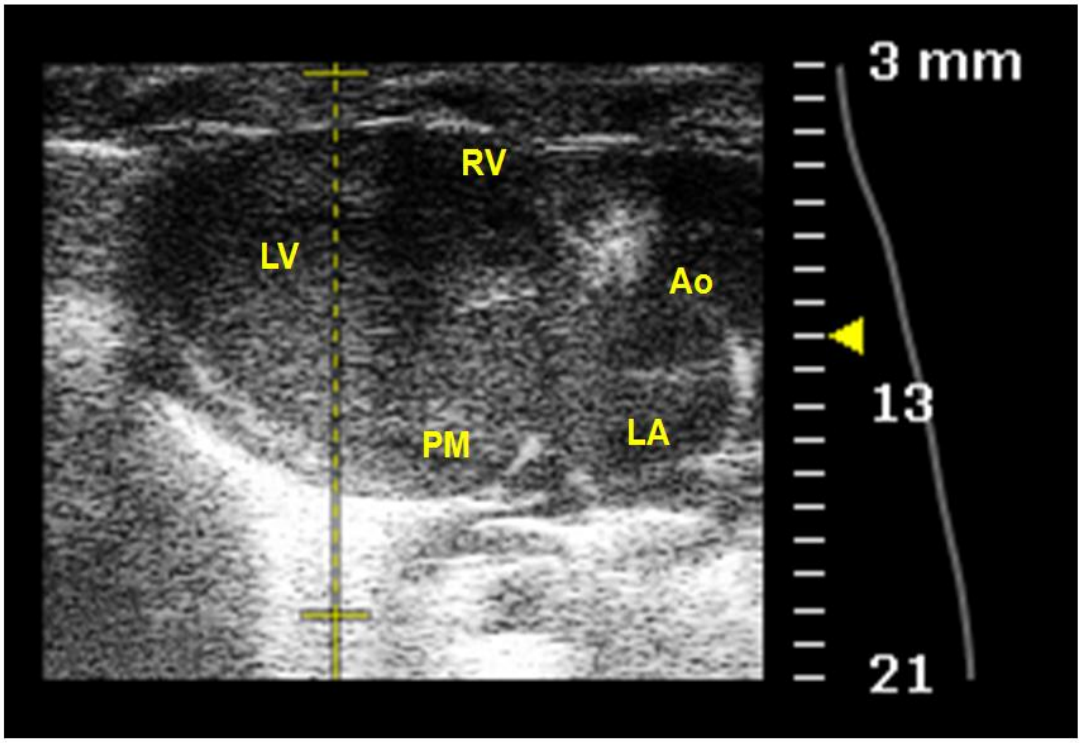

Figure 5. B-mode parasternal long-axis image of the rat heart at the level of the papillary muscle. Images were acquired using the Vevo 2100 ultrasound system (Visualsonics). Ao, aorta; LA, left atrium; LV, left ventricle; PM, papillary muscle; RV, right ventricle.

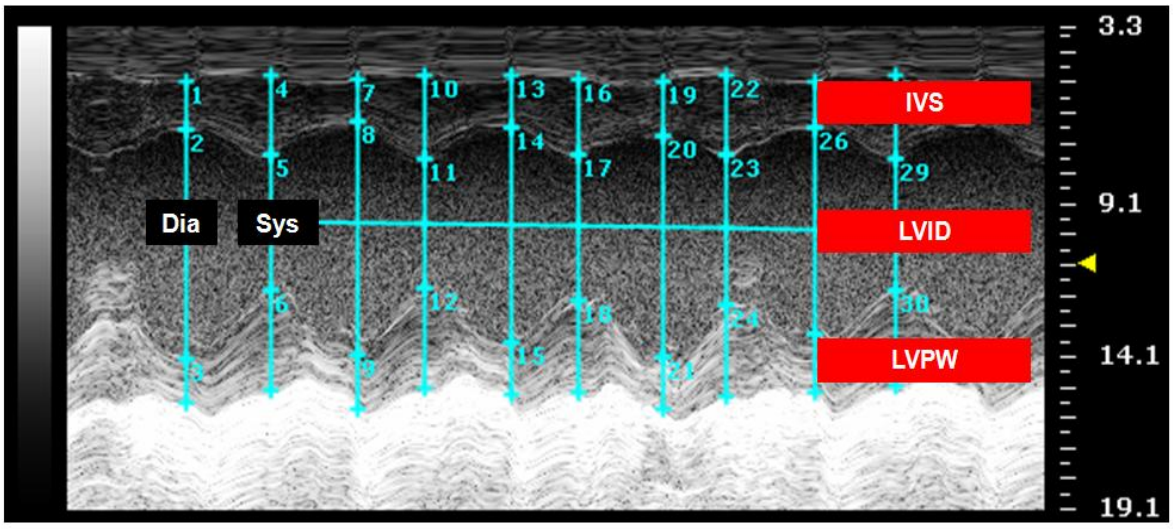

Figure 6 . M-mode parasternal long-axis image of the rat heart at the level of the papillary muscle. Images were acquired using the Vevo 2100 ultrasound system (Visualsonics). Dia, Diastole; IVS, Inter ventricular septum; LVID, Left ventricular internal diameter; LVPW, left ventricular posterior wall; Sys, Systole.

Isolated Rat Heart

Rats were anesthetized using 90mg/mL ketamine and 10mg/mL xylazine, dosed at 0.1 mL/100g body weight. Once animal sensation reflexes, including eye blink, pedal and tail pinch reflexes were absent, the heart was rapidly harvested by midline thoracotomy and placed in ice-cold mitochondrial isolation medium (MIM) buffer for myocardial mitochondrial isolation.

Myocardial Mitochondrial Isolation

Mitochondria were isolated from the LV using a modified protocol (Boehm et al., 2001). From the excised heart, LV was removed, minced, and digested in 10mLs of MIM buffer (300 mmol/L sucrose, 10mmol/L Na-HEPES, and 0.2mmol/L EDTA, pH 7.2) containing 125mg/mL trypsin for 2 minutes and then diluted with trypsin inhibitor medium (10mL of

MIM, pH 7.4, 1mg/mL BSA, and 165mg/mL trypsin inhibitor). The partially digested muscle was suspended in 10mL of MIM containing 1mg/mL BSA and homogenized briefly using a Potter-Elvehjem homogenizer. By differential centrifugation (once at 600 *g* (4°C) for 10 minutes and twice at 8000 *g* (4°C) for 30 minutes, a mitochondrial fraction was obtained as a protein pellet.. The final mitochondrial pellet was suspended in 200uLs of MIM and protein quantification was determined using a Pierce BCA kit.

Mitochondrial Respiration

The respiratory rates of isolated cardiac mitochondria (100 ug) were measured at 25°C in an Oroboros oxygraph in mitochondrial respiration medium (MiR05) (Oroboros Oxygraph-2K, Oroboros Instruments Corp., Innsbruck, Austria). To prevent oxygen limitation, the respiration chambers were hyperoxygenated up to ~400 umol/l O_2. Once oxygen concentration flux stabilized, substrates were added as described in Table 1 and Table 2. The stable portion of the oxygen concentration slope was determined for each addition in both protocols and normalized as in previous respiration studies (Boyle et al., 2011, Anderson et al., 2009).

Table 1. Respirometry protocol A.

Step	Substrate	Notation	Concentration
1	Mitochondria	Mito	100ug
2	Glutamate Malate	G M	5 mM 2 mM
3	ADP	ADP	2 mM
4	Succinate	Succ	5 mM
5	Rotenone	Rot	10 uM
6	FCCP	FCCP	0.75 uM

Protocol A consisted of the following substrate additions: (i) 5 mM glutamate (complex I substrate) + 2 mM malate (complex I substrate), (ii) 2 mM ADP (state 3 condition), (iii) 5 mM succinate (complex II substrate), (iv) 10µM rotenone (inhibitor of complex I), and (v) 0.75 µM carbonylcyanide-*p*-trifluoromethoxyphenylhydrazone (FCCP, a protonophoric uncoupler).

Table 2. Respirometry protocol B.

Step	Substrate	Notation	Concentration
1	Mitochondria	Mito	100ug
2	Palmitoyl carnitine Malate	PC M	25 mM 2 uM
3	ADP	ADP	2 mM
4	Glutamate	Glu	5 mM
5	Succinate	Succ	5 mM
6	FCCP	FCCP	0.75 uM
PC, M: PCM_4 PC, M, ADP: PCM_3			

Protocol B consisted of (i) 25 mM palmitoyl carnitine (fatty acid substrate) + 2 µM malate, (ii) 2 mM ADP, (iii) 5 mM glutamate, (iv) 5 mM succinate, and (v) 0.75 µM FCCP. Specific substrate additions allowed for measurement of state 4 (substrate only, no ADP added), state 3 (ADP), and chemically uncoupled (FCCP) respiration rates. Protocol B observed respiration supported exclusively by lipid (PC) under state 4 (PCM_4) and state 3 (PCM_3). The rate of mitochondrial O2 consumption was expressed as picomoles per second per mg of protein. The respiratory control ratio (RCR) was set as the ratio of oxygen consumption at state 3 over oxygen consumption at state 4.

Statistical analyses

Statistical analyses were performed using commercial software (Prism Software, Irvine, CA) on raw or log-transformed data. For HCR/LCR animal characteristics, t-tests were performed. Analysis of variance with repeated measures was used to compare changes in any echocardiographic parameter over time. Similarly, analysis of variance was used to compare substrate responses in respirometry protocols. Analysis of variance also was used to compare differences between groups at any given time. Specifically, the following comparisons were considered: LCR control vs. HCR Control, LCR Control vs. LCR + DOX, HCR Control vs. DOX, and LCR + DOX vs. HCR + DOX. The following comparisons were considered biologically irrelevant, and were excluded from statistical comparison; LCR Control vs. HCR + DOX, HCR Control vs. LCR + DOX. In each case, data are presented as the mean ± S.E.M. Statistical significance was accepted when $p < 0.05$.

CHAPTER III: RESULTS

Phenotype Characteristics

Animals were characterized as either Low Aerobic Capacity (LCR) running rats, or High Aerobic Capacity (HCR) Running Rats, based on responses to a graded, progressive exercise test. Each rat was run on a motorized treadmill set at 10 m/min on a 15-degree slope, with programmed increases in speed (1 m/min, every 2 min) until the animals reached exhaustion. Rats were tested daily over 5 consecutive days, and the greatest distance run in meters out of the five trials was considered the best estimate of intrinsic exercise capacity. A summary of the demographic data is provided in Table 3.

HCRs had significantly lower body weights (211 ± 3 vs. 158 ± 2 grams, mean ± SEM, LCR vs. HCR, $p < 0.0000$) (figure 7), HCR animals also ran more than 400% longer (78 ± 1 vs. 19 ± 0 minutes, mean ± SEM, HCR vs. LCR, $p < 0.0000$) (figure 8), more than 8 times farther (2276 ± 43 vs. 274 ± 7 meters, mean ± SEM, HCR vs. LCR, $p < 0.0000$) (Figure 9), and achieved running speeds 260% faster (49 ± 1 vs. 19 ± 0 meters, mean ± SEM, LCR vs. HCR, $p < 0.0000$) (Figure 10). Consistent with the possibility that at least some of the running capacity has more to do with behavioral elements, than physiological capacity, LCR animals were significantly less likely to improve with repeated trials. 32% of LCRs vs. only 8% of HCRs ($p < 0.001$, Chi-Square) in this cohort had their best performance on the first trial, while 92% of HCRs had their best performances on the last trial, against only 35% of LCRs ($p < 0.001$, Chi-Square). These data are summarized in (Figure 11)

TABLE 3. Summary of individual BWs and best performances at the time of phenotyping.

	LCRs				HCRs			
	Body wt (g)	**Time (min)**	**Distance (m)**	**Speed (m/min)**	**Body wt (g)**	**Time (min)**	**Distance (m)**	**Speed (m/min)**
	204	21	317	20	149	71	1931	45
	215	18	250	18	139	71	1949	45
	236	14	178	16	156	72	1960	45
	210	18	249	18	154	72	1990	46
	182	14	177	16	189	72	1997	46
	202	20	294	20	172	73	2009	46
	188	20	293	20	148	74	2050	46
	238	22	339	21	160	74	2050	46
	217	18	257	19	172	74	2061	46
	203	20	290	20	168	74	2067	46
	218	16	210	17	139	74	2067	46
	261	17	239	18	150	74	2081	47
	197	20	283	19	172	75	2113	47
	198	20	295	20	154	75	2116	47
	220	18	255	19	163	75	2129	47
	219	20	288	19	178	76	2154	47
	218	18	246	18	157	76	2184	48
	203	15	203	17	174	76	2187	48
	227	21	305	20	161	77	2218	48
	198	19	263	19	146	78	2274	49
	200	21	316	20	157	79	2312	49
	216	20	300	20	148	80	2342	49
	196	21	308	20	141	80	2353	49
	225	19	279	19	157	80	2363	50
	214	20	282	19	168	80	2369	50
	208	21	303	20	155	81	2405	50
	214	21	304	20	173	81	2412	50
	195	22	334	21	165	82	2463	51
	177	17	240	18	157	82	2477	51
	208	21	307	20	161	82	2481	51
	203	18	244	18	156	84	2558	51
	248	19	278	19	157	85	2595	52
	197	17	240	18	147	87	2704	53
	193	21	314	20	140	88	2796	54
	210	20	291	20	161	89	2822	54
	243	20	297	20	143	90	2884	55
mean	211	19	274	19	158	78	2276	49
SEM	3	0	7	0	2	1	43	0
p	0.0000	0.0000	0.0000	0.0000				

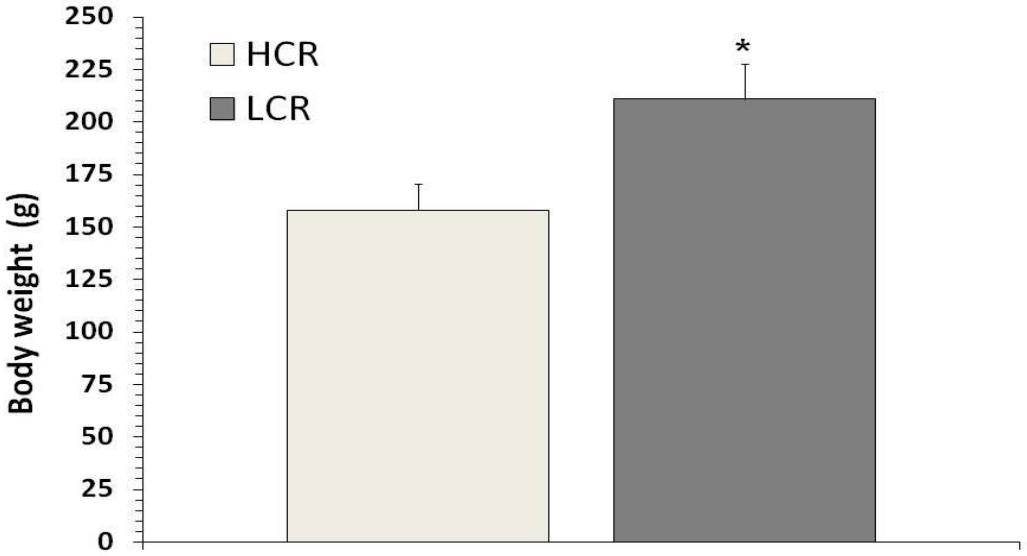

Figure 7. Summary of body weight differences between HCR and LCR cohorts at the time of phenotyping (12 weeks of age). * indicates p< 0.05 vs. HCR

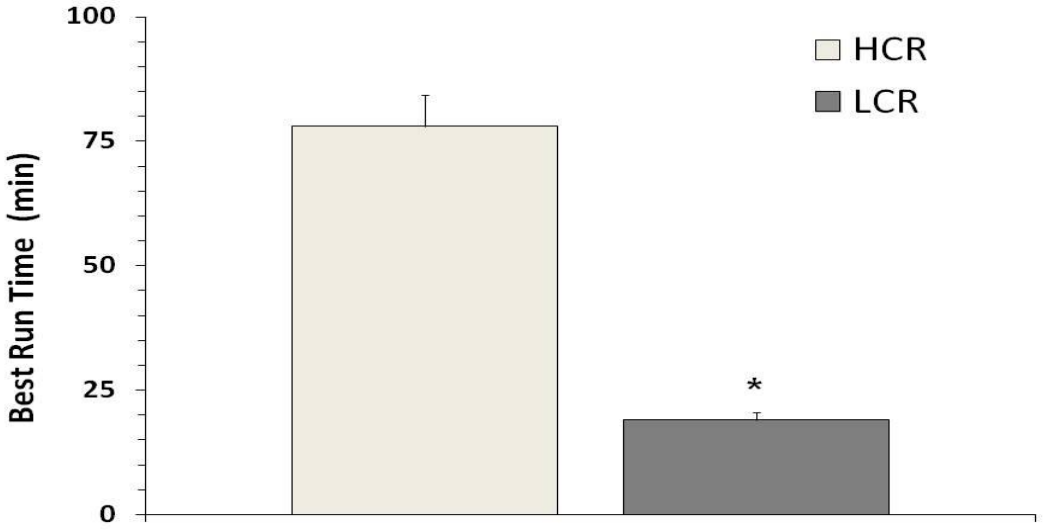

Figure 8. Summary of best run times in the HCR and LCR cohorts at the time of phenotyping (12 weeks of age). * indicates p< 0.05 vs. HCR

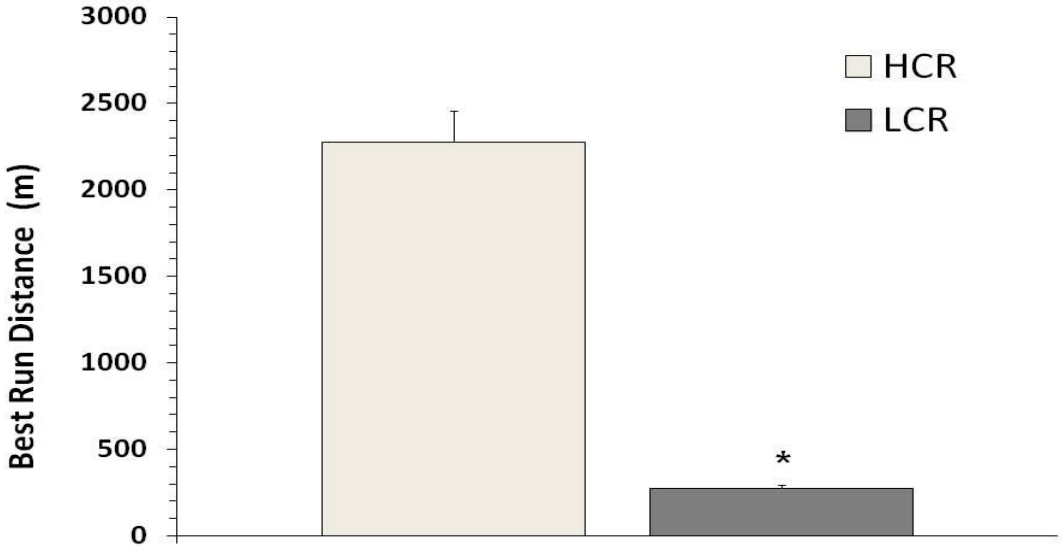

Figure 9. Summary of best run distances HCR and LCR cohorts at the time of phenotyping (12 weeks of age). * indicates p< 0.05 vs. HCR

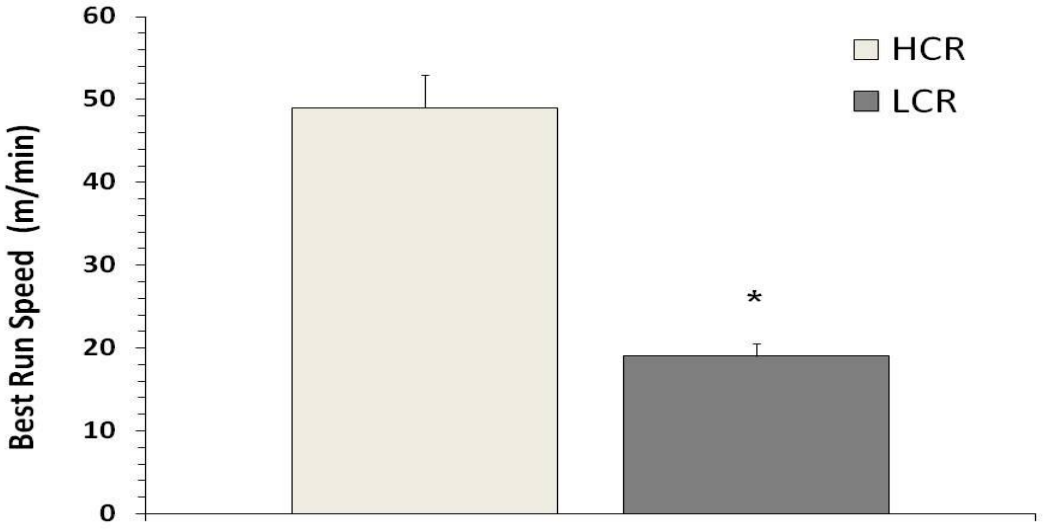

Figure 10. Summary of best run speeds in HCR and LCR cohorts at the time of phenotyping (12 weeks of age). * indicates p< 0.05 vs. HCR

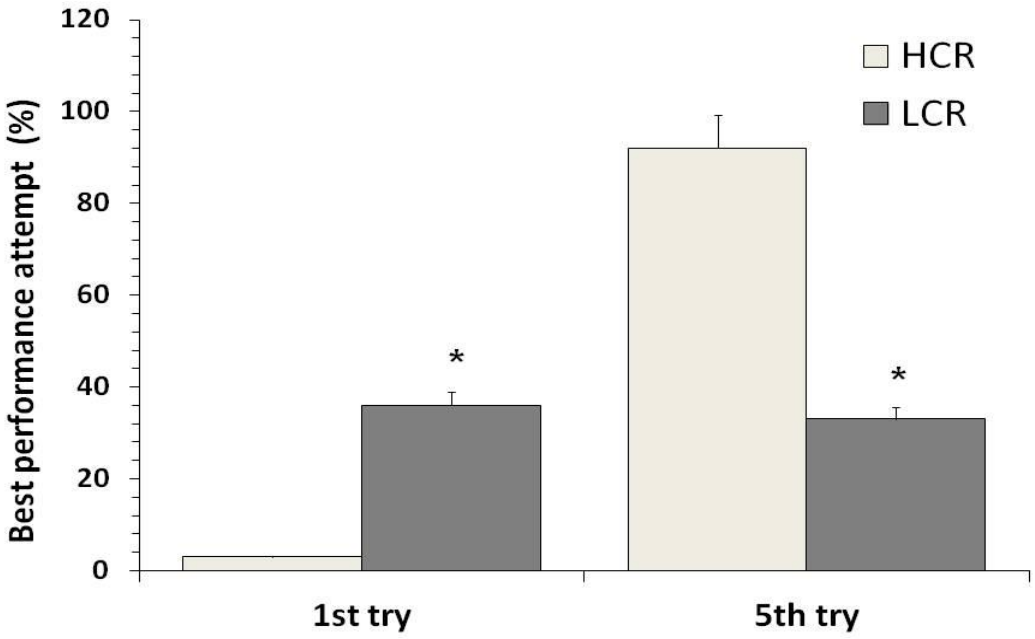

Figure 11. Summary of best performance trial (1-5) in the HCR and LCR cohorts at the time of phenotyping (12 weeks of age). * indicates $p < 0.05$ vs. HCR

Echocardiographic Assessment

Control Comparisons

In general, there were no statistical differences overall under control conditions between HCR and LCR animals. HCR animals tended to operate with higher end diastolic volumes (Table 4, Figure 12), end systolic volumes (Table 5, Figure 13), stroke volumes (Table 6, Figure 14) cardiac outputs (Table 7, Figure 15) and heart rates (Table 8, Figure 16). The picture is consistent with an increased overall hyperdynamic hemodynamic state, but also with a picture that no one variable in cardiac performance can explain the differences in performance in aerobic performance. The ejection fractions (Table 9, Figure 18), were essentially identical between groups, and therefore, a significant difference in intrinsic

cardiac contractility likely does not explain the overall difference in performance. However, it is possible that the present results simply represent the residual vestige effects of a larger difference that may have been present at earlier ages.

TABLE 4. Summary of left ventricular end-diastolic volume (LVEDV) changes by phenotype.

	LVEDV (uL)				
	day 0	**day 1**	**day 4**	**day 7**	**day 10**
HCR	162	185	216	199	212
Control	223	233	233	284	305
	315	268	321	371	223
mean	233	229	257	285	247
SEM	36	20	27	40	24
p vs day 0		0.4236	0.1050	0.1719	0.2799
LCR	209	245	176	98	223
Control	173	153	168	311	307
	247	264	300	275	202
	271	205	279	238	199
	161	114	171	182	208
	168	168	171	175	204
mean	205	162	207	198	204
SEM	19	22	29	16	2
p vs day 0		0.2175	0.1960	0.4677	0.3597
p vs HCR	0.2493	0.1779	0.1559	0.1229	0.2473

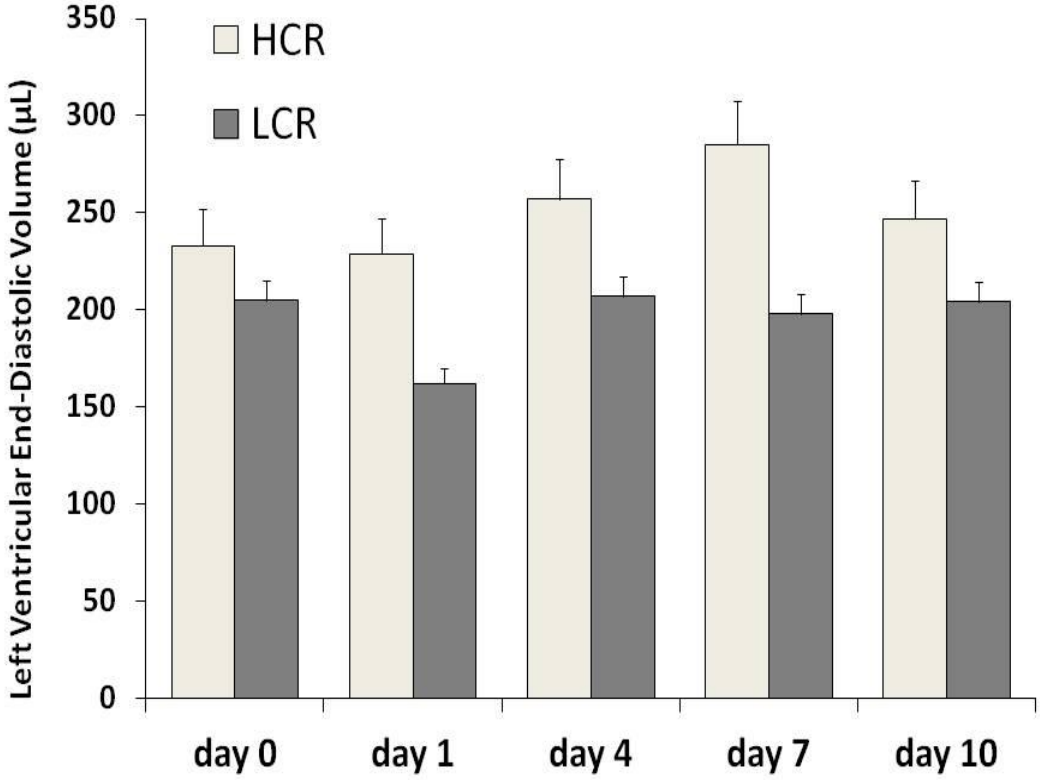

Figure 12. **Summary of diastolic ventricular chamber size by phenotype.**

TABLE 5. Summary of left ventricular end systolic volume (LVESV) changes by phenotype.

	LVESV (uL)				
	day 0	**day 1**	**day 4**	**day 7**	**day 10**
HCR	49	51	56	55	48
Control	66	73	75	83	79
	95	89	88	97	58
mean	70	71	73	78	62
SEM	11	9	8	10	7
p vs day 0		0.4082	0.1838	0.1177	0.1376
LCR	71	44	49	32	71
Control	42	33	43	107	93
	71	90	96	86	79
	94	45	68	68	42
	36	37	39	46	50
	36	36	29	39	50
mean	58	39	45	51	47
SEM	10	2	10	7	2
p vs day 0		0.1592	0.0842	0.2393	0.4523
p vs HCR	0.2540	0.0764	0.1335	0.2268	0.4283

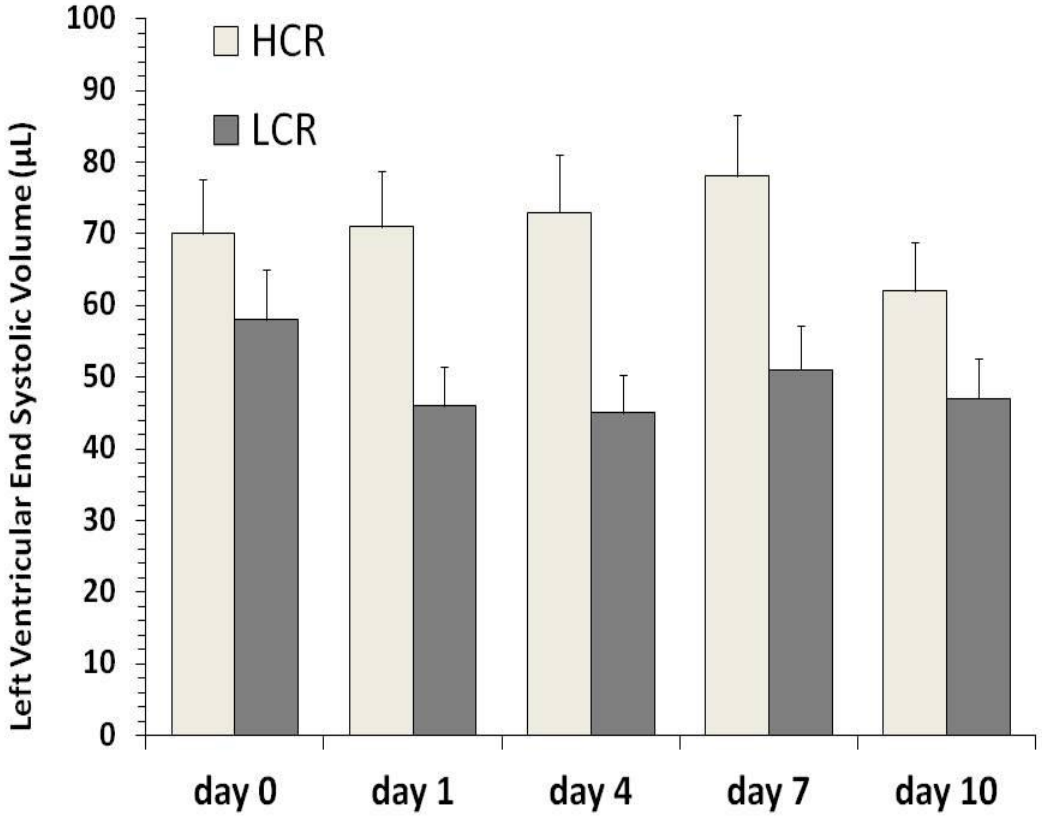

Figure 13. **Summary of systolic chamber size by phenotype.**

TABLE 6. Summary of left ventricular stroke volume (LV SV) changes by phenotype.

	LV SV (uL)				
	day 0	**day 1**	**day 4**	**day 7**	**day 10**
HCR	113	134	160	144	164
Control	157	160	158	201	226
	220	179	233	274	165
mean	163	158	184	206	185
SEM	25	11	20	31	17
p vs day 0		0.3933	0.1244	0.1837	0.3365
LCR	138	201	127	66	152
Control	131	120	125	204	214
	176	174	204	189	123
	178	160	211	170	157
	125	77	132	136	158
	132	132	142	136	154
mean	145	123	161	147	156
SEM	14	20	20	9	1
p vs day 0		0.4337	0.2682	0.3806	0.3304
p vs HCR	0.2593	0.3170	0.1875	0.0943	0.1481

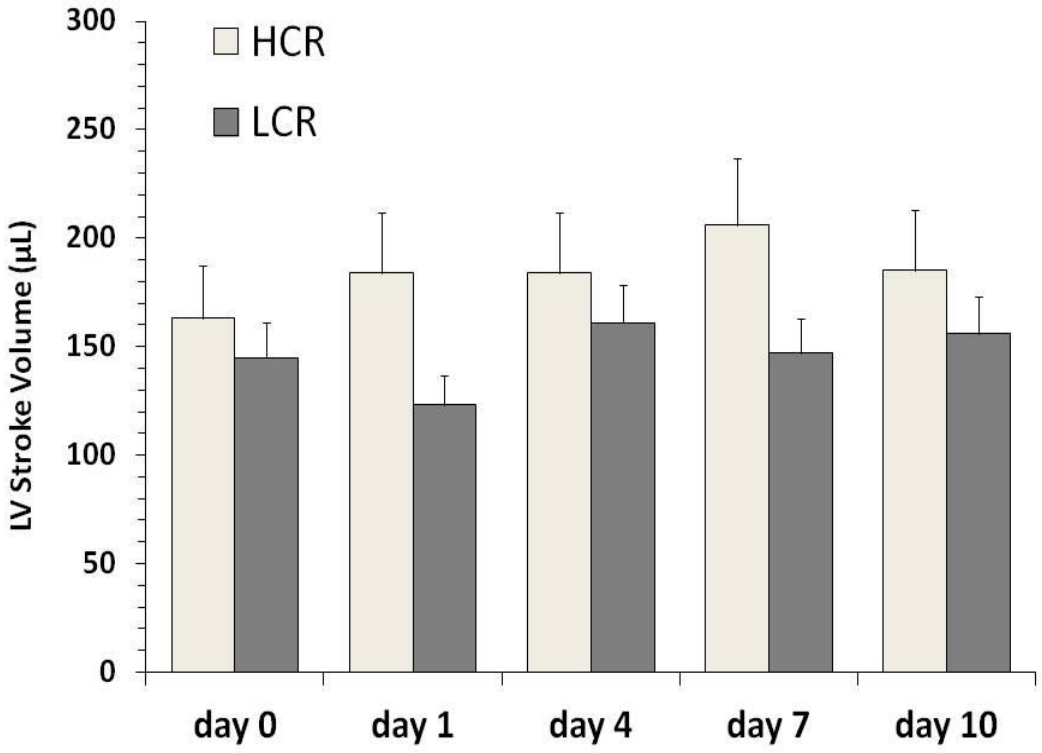

Figure 14. **Summary of left ventricular stroke volume (LV SV) changes by phenotype.**

TABLE 7. Summary of heart rate (Rate) changes by phenotype.

	Rate (bpm)				
	day 0	**day 1**	**day 4**	**day 7**	**day 10**
HCR	325	365	335	362	269
Control	341	315	343	347	348
	318	326	316	337	302
mean	328	335	331	349	306
SEM	6	12	7	6	19
p vs day 0		0.3687	0.4180	0.0641	0.1311
LCR	345	250	356	359	348
Control	345	334	323	316	313
	387	402	368	371	336
	270	340	372	338	310
	336	300	328	336	312
	330	342	345	312	319
mean	312	327	348	329	314
SEM	17	11	10	7	2
p vs day 0		0.3769	0.1723	0.1252	0.0313
p vs HCR	0.3771	0.4119	0.1160	0.2585	0.1879

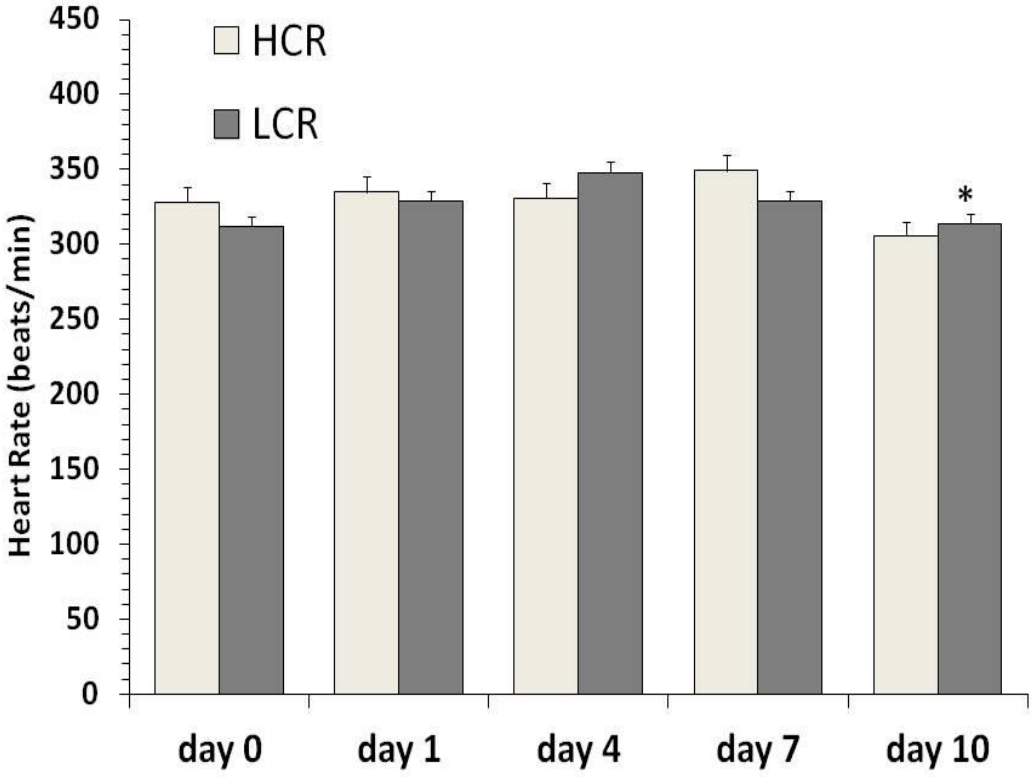

Figure 15. **Summary of heart rate (Rate) changes by phenotype.** * $p < 0.05$ vs. day zero value.

TABLE 8. Summary of left ventricular cardiac output (CO) changes by phenotype.

	CO (ul/min/g)				
	day 0	**day 1**	**day 4**	**day 7**	**day 10**
HCR	123	165	146	192	162
Control	198	162	166	203	244
	176	170	149	146	144
mean	166	166	154	180	183
SEM	18	2	5	14	25
p vs day 0		0.5000	0.1366	0.1093	0.4489
LCR	91	116	106	72	122
Control	128	97	100	147	156
	157	162	175	167	100
	104	137	178	130	109
	147	51	134	145	157
	174	182	161	141	197
mean	142	123	158	139	154
SEM	17	31	10	4	21
p vs day 0		0.3265	0.1485	0.2803	0.3714
p vs HCR	0.1109	0.0923	0.3020	0.0386	0.0948

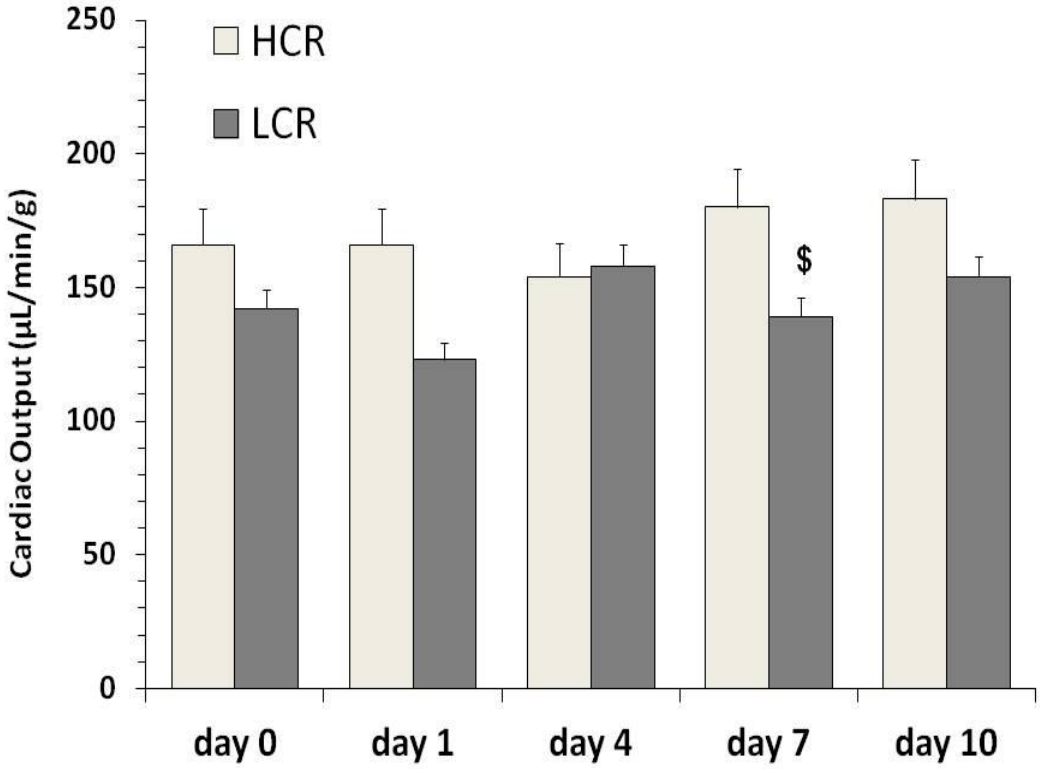

Figure 16. Summary of left ventricular cardiac output (CO) changes by phenotype.

$ $p < 0.05$ vs. HCR value at the same time point.

TABLE 9. Summary of left ventricular ejection fraction (LV EF) changes by phenotype.

	LV EF (%)				
	day 0	**day 1**	**day 4**	**day 7**	**day 10**
HCR	70	72	74	72	77
Control	70	69	68	71	74
	70	67	73	74	74
mean	70	69	71	72	75
SEM	0	1	2	1	1
p vs day 0		0.3619	0.1875	0.3063	0.0923
LCR	66	82	72	67	68
Control	76	78	74	66	70
	71	66	68	69	61
	65	78	76	71	79
	78	68	77	75	76
	79	79	83	78	75
mean	74	75	79	75	77
SEM	3	3	2	1	1
p vs day 0		0.2740	0.4951	0.0124	0.3993
p vs HCR	0.2523	0.1011	0.1562	0.3180	0.1979

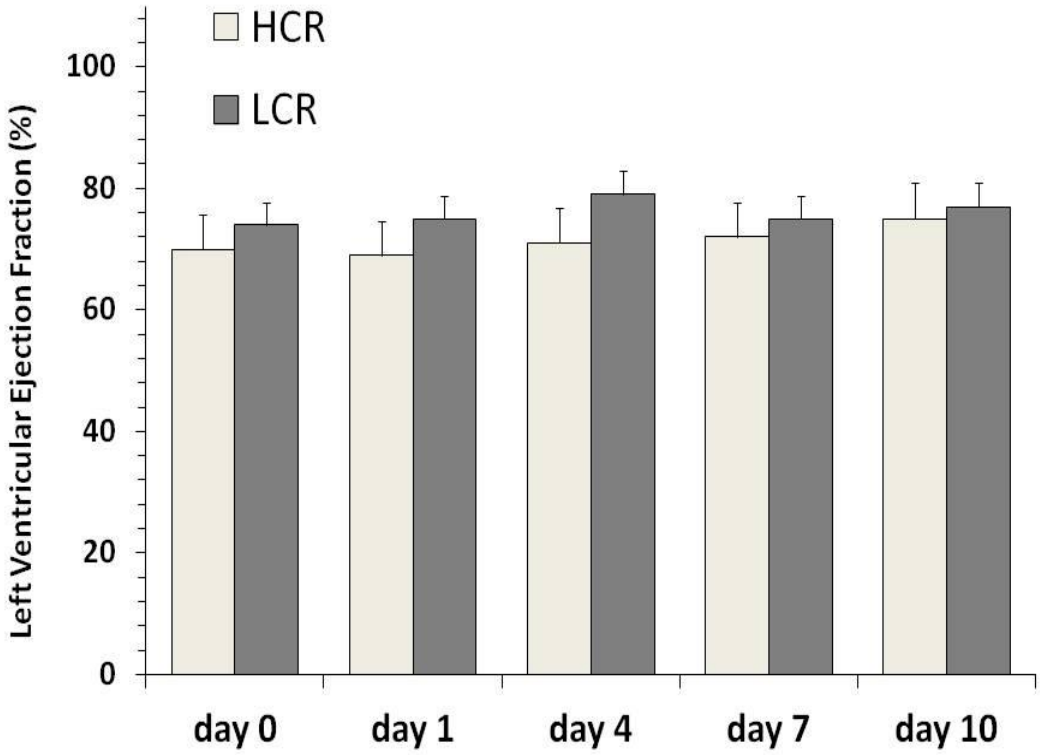

Figure 17. **Summary of left ventricular ejection fraction (LV EF) changes by phenotype.**

Phenotypic responses to Doxorubicin

Doxorubicin treatment had no real effect on end-diastolic volume in the HCR animals, but end-diastolic volume increased significantly in the LCR animals (Table 10, Figures 18, 19). Similarly, end systolic volumes in the left ventricle also tended to increase significantly in the LCR animals, but not in the HCRs (Table 11, Figures 20, 21). The data are consistent with a mild loss of function in the LCR animals in the first 4-7 days.

TABLE 10. Summary of left ventricular end-diastolic volume (LVEDV) changes caused by doxorubicin treatment in each phenotype.

	LVEDV (uL)				
	day 0	**day 1**	**day 4**	**day 7**	**day 10**
HCR + Dox	106	226	240	143	288
	252	187	247	250	204
	187	238	191	199	240
	335	238	392	250	399
	110	210	197	243	113
mean	198	220	253	217	249
SEM	44	10	36	21	47
p vs day 0		0.3215	0.1946	0.1813	0.2946
p vs HCR	0.0804	0.1396	0.4600	0.1340	0.4870
LCR + Dox	223	231	307	213	275
	178	163	301	110	194
	279	279	290	252	339
	250	301	325	315	329
	205	212	236	214	277
	187	153	259	243	169
	197	216	178	268	175
	208	225	197	191	225
mean	216	223	262	226	248
SEM	12	18	19	21	24
p vs day 0		0.2394	0.0599	0.1241	0.1995
p vs LCR	0.3654	0.0000	0.0000	0.0000	0.0000
p vs. HCR D	0.3177	0.4566	0.4145	0.3943	0.4924

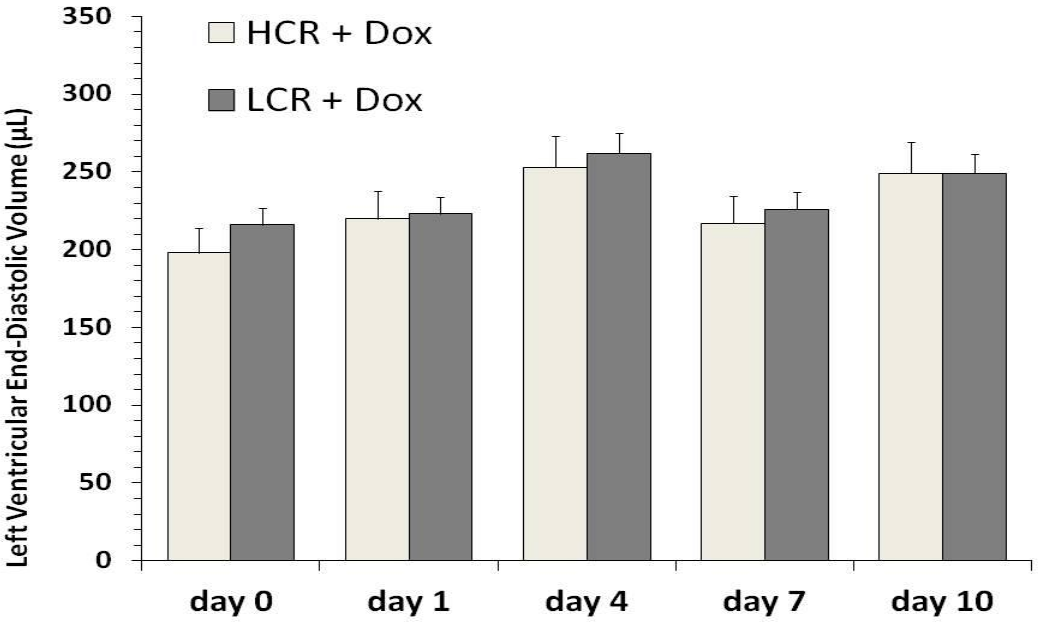

Figure 18. Summary of left ventricular end-diastolic volume (LVEDV) changes caused by doxorubicin treatment in each phenotype.

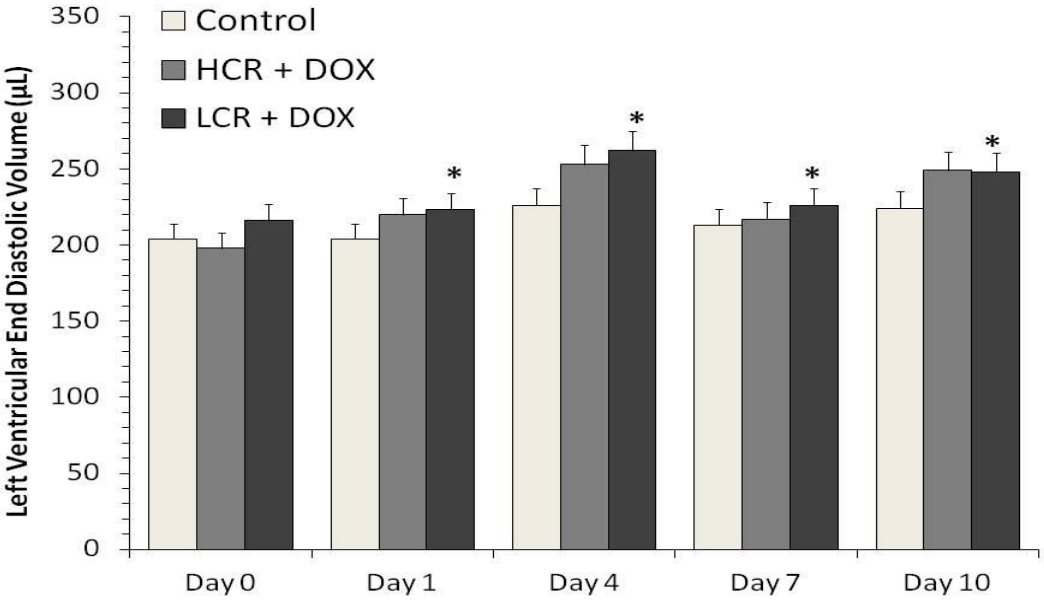

Figure 19. Summary of Doxorubicin effect compared to control in each phenotype.
* $p < 0.05$ vs. control value at each time point.

TABLE 11. Summary of left ventricular end-systolic volume (LVESV) changes caused by doxorubicin treatment in each phenotype.

	LVESV (uL)				
	day 0	**day 1**	**day 4**	**day 7**	**day 10**
HCR + Dox	32	74	71	51	104
	62	86	83	109	57
	91	83	79	52	96
	155	92	202	111	212
	29	87	59	88	39
mean	74	84	99	82	102
SEM	23	3	26	13	30
p vs day 0		0.3230	0.2932	0.2449	0.2774
p vs HCR	0.4215	0.0539	0.0510	0.1490	0.0537
LCR + Dox	33	75	78	39	36
	50	37	110	29	69
	20	64	68	107	115
	27	76	76	104	123
	51	49	64	59	94
	55	48	52	67	49
	36	33	72	52	37
	36	81	47	20	40
mean	38	58	71	60	70
SEM	4	7	7	11	13
p vs day 0		0.0437	0.1402	0.2218	0.1016
p vs LCR	0.0161	0.4808	0.0702	0.4143	0.1102
p vs. HCR D	0.0429	0.0058	0.1143	0.1155	0.1468

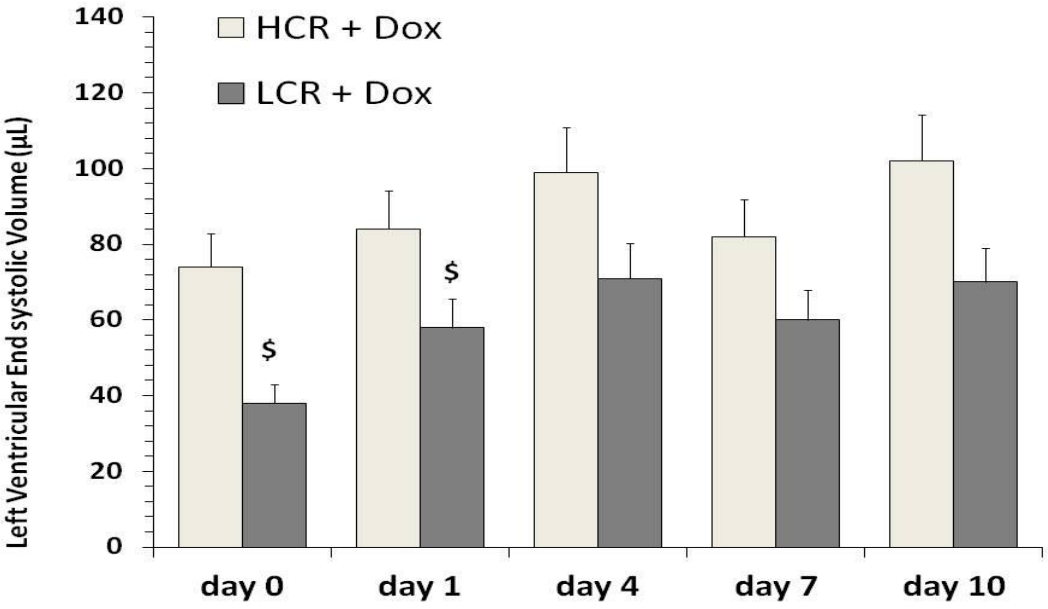

Figure 20. Summary of left ventricular end-systolic volume (LVESV) changes caused by doxorubicin treatment in each phenotype. $ $p < 0.05$ vs. HCR phenotype at the same time point.

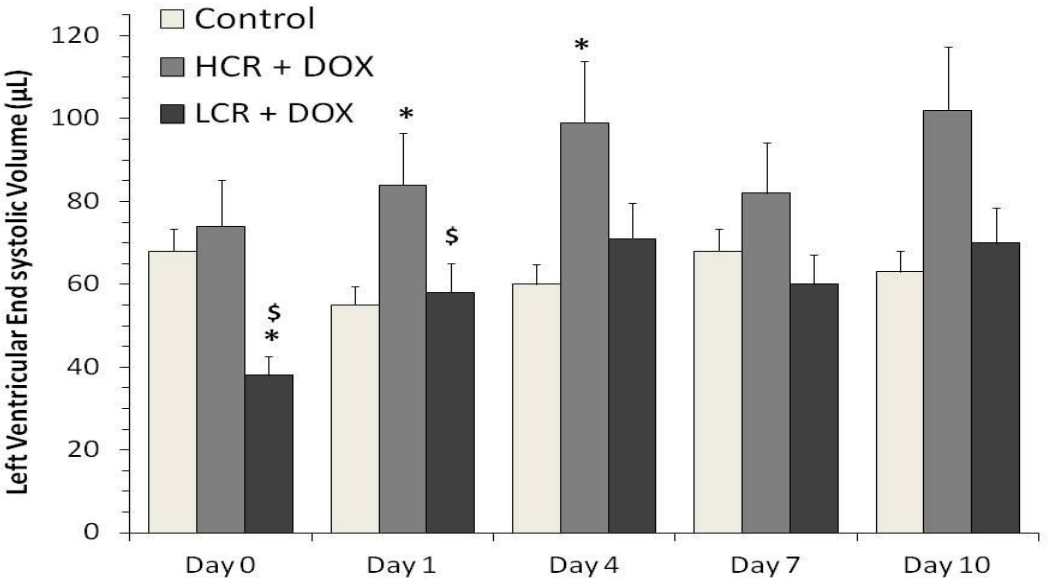

Figure 21. Summary of Doxorubicin effect compared to control on left ventricular end-systolic volume (LVESV) in each phenotype. * $p < 0.05$ vs. control value at each time point. $ $p < 0.05$ vs. HCR phenotype at the same time point.

Doxorubicin treatment was associated with a decreasing stroke volume in the HCR animals, while stroke volume tended to increase in the LCRS, consistent with the increased overall volumes observed in these animals (Table 12, Figures 22, 23). The changes were seen variably over the entire 10 day observation period, consistent with a system under stress.

TABLE 12. Summary of left ventricular stroke volume (LV SV) changes caused by doxorubicin treatment in each phenotype.

	LV SV (uL)				
	day 0	**day 1**	**day 4**	**day 7**	**day 10**
HCR + DOX	74	152	169	92	184
	190	101	164	141	147
	96	155	112	147	144
	180	146	190	139	187
	81	123	138	155	74
mean	124	135	155	135	147
SEM	25	10	13	11	20
p vs day 0		0.3690	0.1722	0.1970	0.3446
p vs HCR	0.0167	0.0228	0.1277	0.0220	0.0863
LCR + DOX	190	156	229	174	239
	128	126	191	81	125
	259	215	222	145	224
	223	225	249	211	206
	154	163	172	155	183
	132	105	207	176	120
	161	183	106	216	138
	173	144	150	171	185
mean	177	165	191	166	178
SEM	16	15	17	15	16
p vs day 0		0.0834	0.1105	0.1666	0.2903
p vs LCR	0.0469	0.1883	0.0072	0.1639	0.0468
p vs. HCR D	0.0424	0.0906	0.0773	0.0821	0.1337

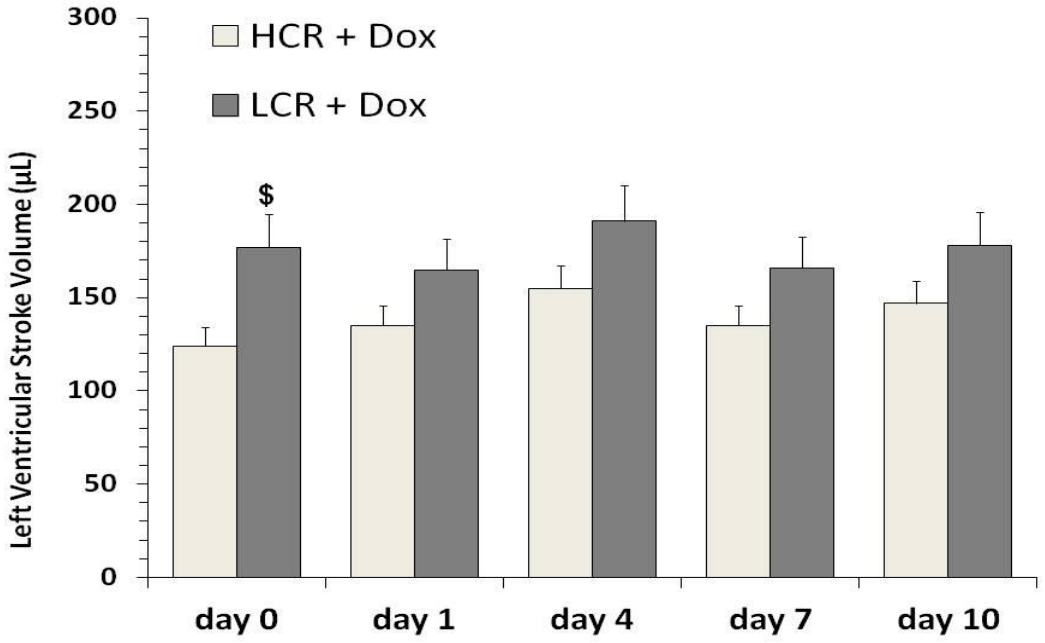

Figure 22. Summary of left ventricular end-systolic volume (LVESV) changes caused by doxorubicin treatment in each phenotype.

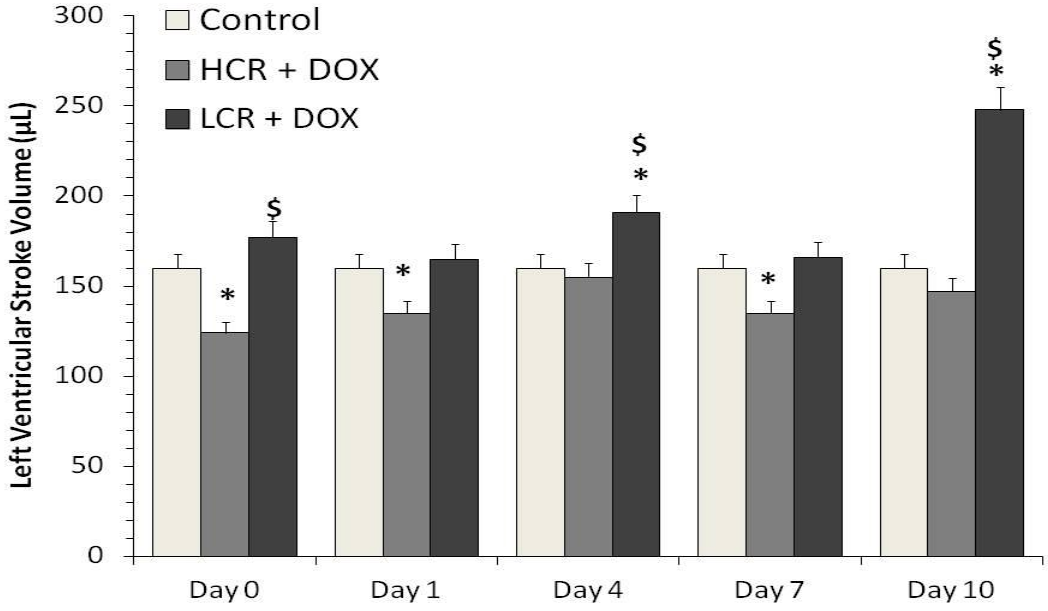

<u>Figure 23.</u> Summary of Doxorubicin effect on stroke volume compared to control in each phenotype. * $p < 0.05$ vs. control value at each time point. $ $p < 0.05$ vs. HCR phenotype at the same time point.

In contrast to the stroke volume changes, reciprocal patterns were seen in the heart rate responses. The HCR animals tended to have increased heart rates in response to doxorubicin treatment, while the LCRS tended to show decreasing rate patterns. The increased heart rates in the HCRs were significantly increased throughout the treatment period, while the decrease in hear rate in the LCRs abated within 7 days after treatment began (Table 13, Figures 24, 25).

TABLE 13. Summary of heart rate (Rate) changes caused by doxorubicin treatment in each phenotype.

	Rate (bpm)				
	day 0	**day 1**	**day 4**	**day 7**	**day 10**
HCR + DOX	374	336	343	376	352
	393	326	381	380	340
	307	326	381	370	333
	345	386	421	377	377
	357	370	532	301	366
mean	355	349	412	361	354
SEM	15	12	33	15	8
p vs day 0		0.3821	0.0377	0.1689	0.3645
p vs HCR	0.0399	0.0811	0.0005	0.0190	0.0314
LCR + DOX	337	277	295	344	336
	306	308	308	309	332
	296	311	276	320	324
	375	315	314	369	332
	245	262	327	358	305
	338	439	328	336	337
	353	317	349	353	345
	315	242	23	285	318
mean	321	309	278	334	329
SEM	14	21	37	10	4
p vs day 0		0.2921	0.1834	0.0514	0.2971
p vs LCR	0.1455	0.0495	0.0059	0.4858	0.2981
p vs. HCR D	0.0663	0.0954	0.0152	0.0754	0.0066

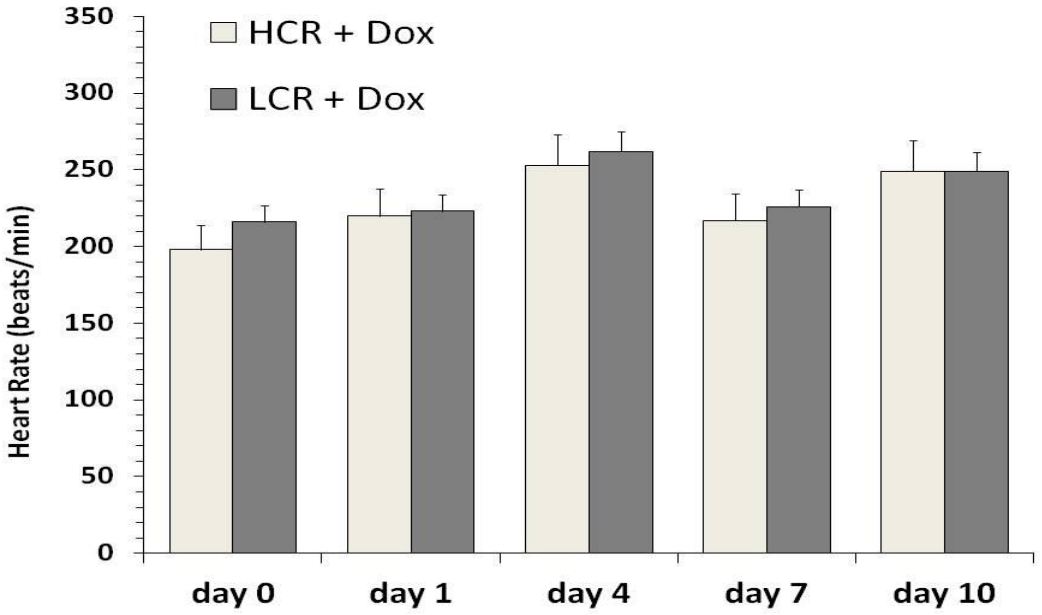

Figure 24. Summary of left ventricular end-systolic volume (LVESV) changes caused by doxorubicin treatment in each phenotype.

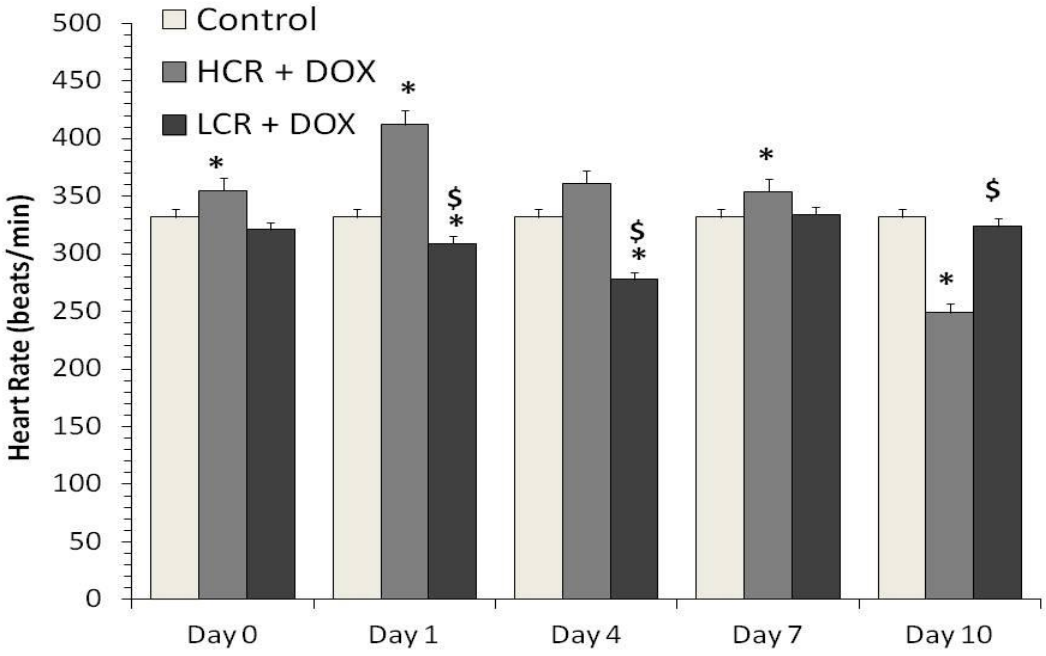

Figure 25. Summary of Doxorubicin effect on heart rate compared to control in each phenotype. * $p < 0.05$ vs. control value at each time point. $ $p < 0.05$ vs. HCR phenotype at the same time point.

Cardiac output is the product of heart rate and stroke volume. The aggregate effects of doxorubicin treatment on the HCRs were an increase in total output that was significant by Day 7 after treatment. In LCR animals, doxorubicin treatment tended to increase output early after treatment, but only weakly so, and cardiac output was consistently reduced compared to the HCR animals (Table 14, Figures 26, 27).

TABLE 14. Summary of cardiac output (CO) changes caused by doxorubicin treatment in each phenotype.

	CO (ul/min/g)				
	day 0	**day 1**	**day4**	**day 7**	**day 10**
HCR + DOX	107.33	199.23	245.54	151.66	284.49
	298.03	132.70	260.23	68.01	219.68
	113.72	200.78	178.05	224.36	196.60
	255.76	238.34	275.73	218.54	283.59
	108.30	182.65	196.04	189.25	107.76
mean	177	191	231	170	218
SEM	41	17	19	29	33
p vs day 0		0.3940	0.0898	0.1039	0.1735
p vs HCR	0.0830	0.1100	0.4459	0.0496	0.3271
LCR + DOX	153	106	168	157	212
	121	125	196	87	157
	147	134	130	100	161
	223	190	214	216	191
	91	104	139	140	143
	103	86	161	144	102
	119	123	79	166	105
	163	105	109	152	184
mean	140	122	150	145	157
SEM	15	11	16	14	14
p vs day 0		0.0420	0.0498	0.4227	0.2679
p vs LCR	0.2656	0.2222	0.0984	0.1492	0.0308
p vs. HCR D	0.1718	0.0023	0.0037	0.2002	0.0358

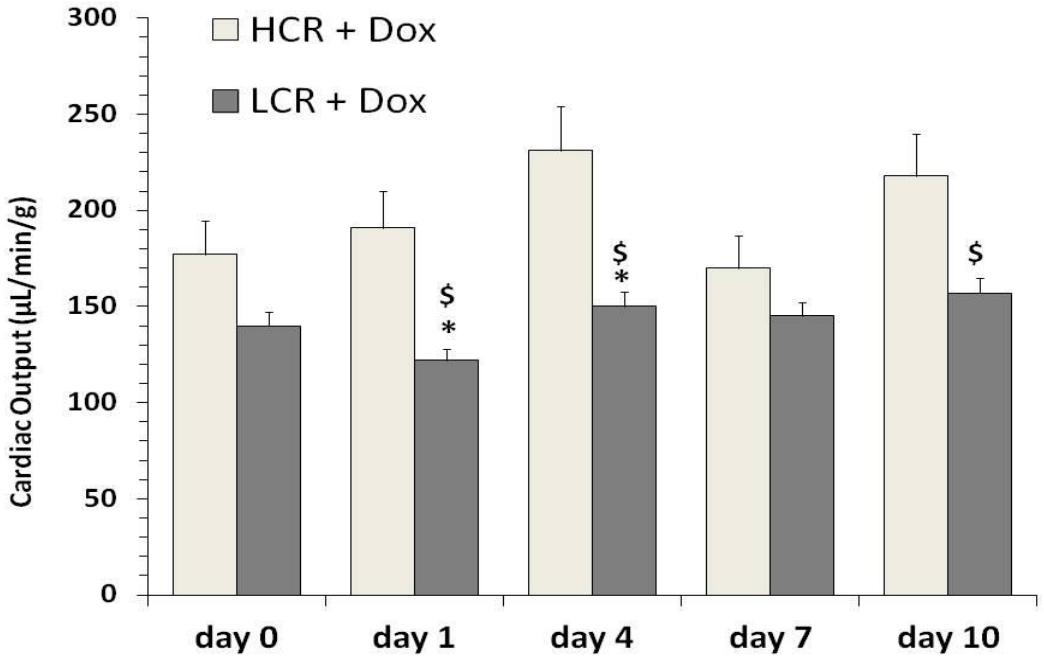

Figure 26. Summary of left ventricular cardiac output (CO) changes caused by doxorubicin treatment in each phenotype.

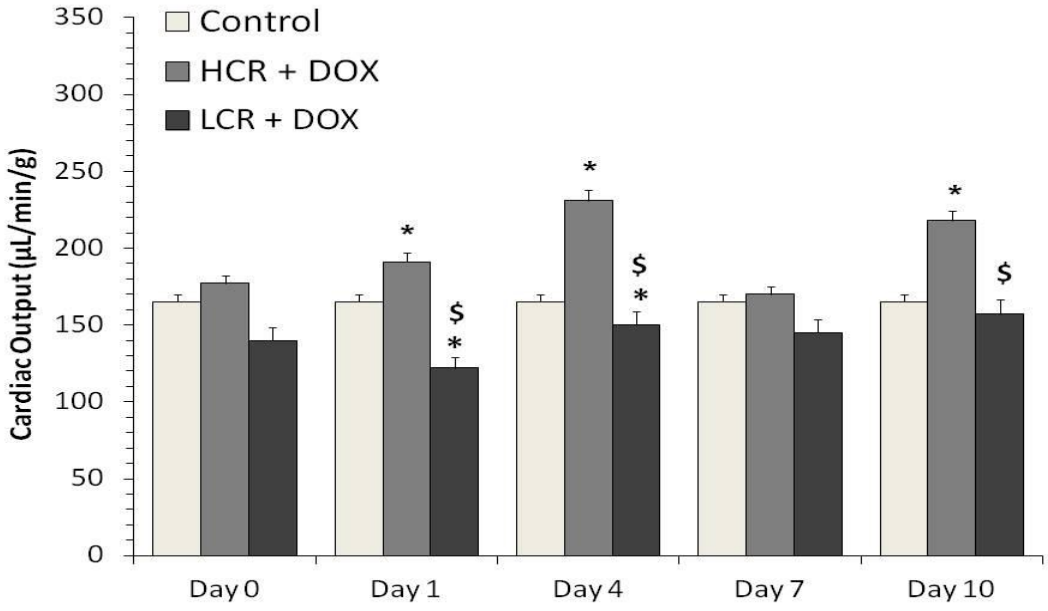

Figure 27. Summary of Doxorubicin effect on cardiac output compared to control in each phenotype. * $p < 0.05$ vs. control value at each time point. $ $p < 0.05$ vs. HCR phenotype at the same time point.

Ejection fraction decreased at all times in the HCR animals following treatment with doxorubicin, consistent with a decrease in contractility, but did not change at any time after treatment in the LCRs. The differences in response to doxorubicin treatment remained significant throughout the first week, but had normalized by ten days (Table 15, Figures 28, 29).

TABLE 15. Summary of left ventricular ejection fraction (LV EF) changes caused by doxorubicin treatment in each phenotype.

	LV EF (%)				
	day 0	**day 1**	**day 4**	**day 7**	**day 10**
HCR + DOX	70	67	70	64	64
	75	54	66	56	72
	51	65	59	74	60
	54	61	48	56	47
	73	59	70	64	65
mean	65	61	63	63	62
SEM	5	2	4	3	4
p vs day 0		0.3111	0.3863	0.4997	0.4164
p vs HCR	0.0189	0.0000	0.0016	0.0004	0.0006
LCR + DOX	85	68	75	82	87
	72	77	63	74	64
	93	77	77	58	66
	89	75	77	67	63
	75	77	73	72	66
	71	69	80	72	71
	82	85	60	81	79
	83	64	76	90	82
mean	81	74	72	74	72
SEM	3	2	3	3	3
p vs day 0		0.0418	0.3837	0.3510	0.1866
p vs LCR	0.0010	0.3531	0.4151	0.3024	0.3933
p vs. HCR D	0.0054	0.0023	0.0286	0.0226	0.0345

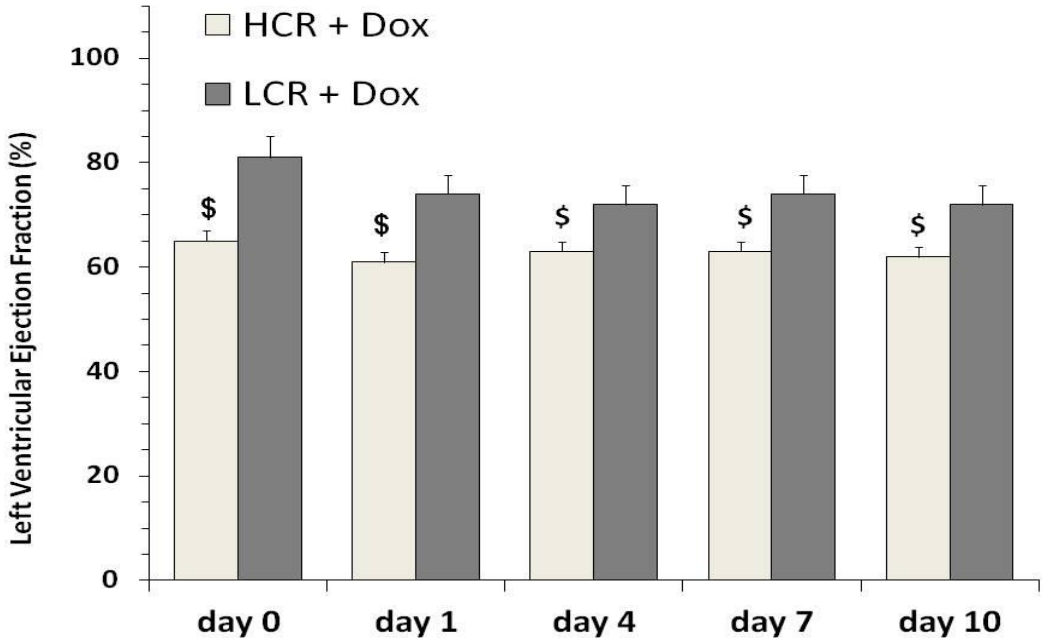

Figure 28. Summary of left ventricular ejection fraction (LV EF) changes caused by doxorubicin treatment in each phenotype. $ $p < 0.05$ vs. HCR phenotype at the same time point.

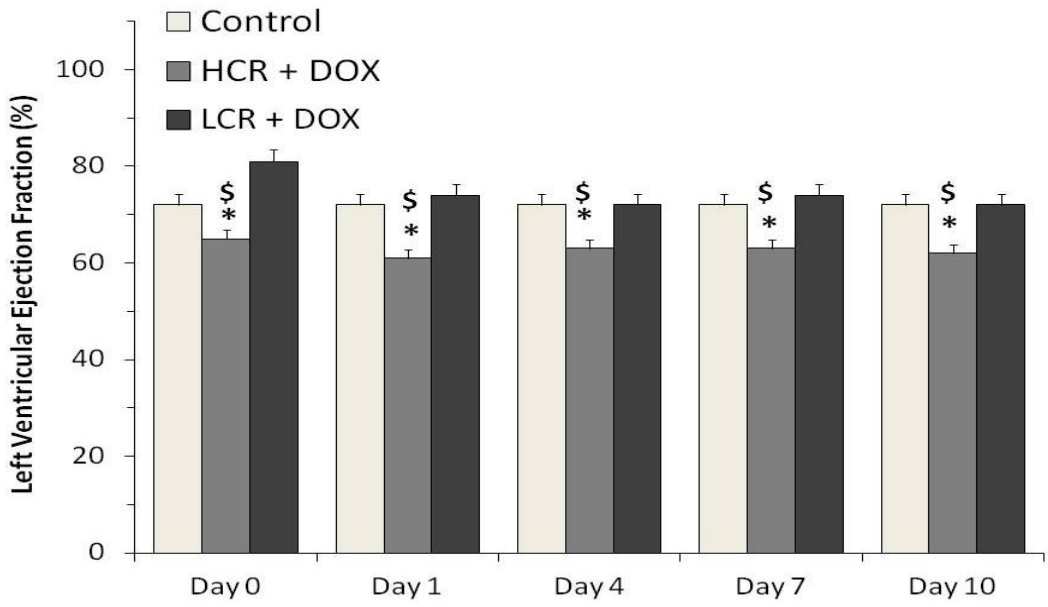

Figure 29. Summary of Doxorubicin effect on ejection fraction compared to control in each phenotype. * $p < 0.05$ vs. control value at each time point. $ $p < 0.05$ vs. HCR phenotype at the same time point.

Mitochodrial Respiratory Capacity

Increases in oxygen consumption above baseline were seen with the addition of ADP, and with subsequent addition of succinate in the glutamate malate protocol. Values for oxygen consumption are consistent with those reported in isolated fibers from young rat, and there were no differences between the phenotypes, suggesting that there was no age dependent decrement in cardiac mitochondrial function, and no impact of phenoptype on that outcome. (Table 16, Figure 30).

TABLE 16. Summary of oxygen consumption data under Glutamate/Malate protocol conditions, obtained using cardiac mitochondria isolated from aged HCR and LCR animals.

	Condition					
Group	**baseline**	**G/M**	**ADP**	**SUCC**	**ROT**	**FCCP**
HCR	377.9	528.9	860.0	1516.2	1016.7	991.6
	12.6	50.9	290.1	545.2	334.6	289.7
	78.8	96.0	159.6	229.9	198.9	192.2
mean	156.4	225.3	436.6	763.8	516.7	491.2
SEM	112.4	152.4	215.0	387.1	253.0	251.8
p vs. Baseline		0.3633	0.0466	0.0112	0.0270	0.0354
p vs. Previous			0.0573	0.0995	0.1060	0.0733
LCR	379.7	636.5	790.9	1064.1	896.9	960.0
	103.3	118.0	418.7	787.1	430.7	441.9
	128.1	178.7	527.1	759.2	427.9	425.2
	232.4	284.0	711.5	1002.2	579.8	527.1
	231.3	249.5	503.9	729.8	423.8	390.8
	126.6	175.6	418.5	664.9	456.5	399.9
mean	200.2	273.7	561.8	834.5	535.9	524.2
SEM	42.5	76.4	63.4	65.4	76.1	89.4
p vs Baseline		0.1490	0.0001	0.0000	0.0004	0.0011
p vs. Previous			0.0003	0.0000	0.0003	0.2773
p vs HCR	0.3715	0.3972	0.3125	0.4364	0.4739	0.4555

Baseline; oxygen consumption with only mitochondria and buffer; **G/M**, oxygen consumption with subsequent addition of Glutamate /malate; **ADP**, oxygen consumption with subsequent addition of ADP; **SUCC**, oxygen consumption with subsequent addition of succinate; **ROT**, oxygen consumption with subsequent addition of Rotenone; **FCCP**, oxygen consumption with subsequent addition of carbonylcyanide-*p*-trifluoromethoxyphenylhydrazone

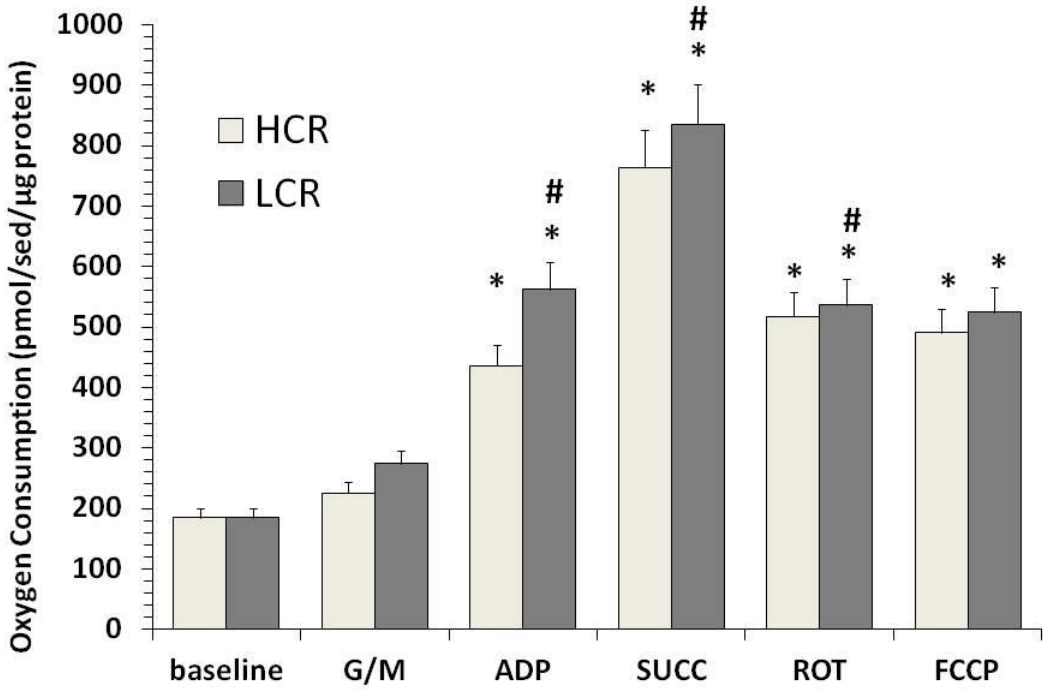

<u>Figure 30</u>. Comparison of phenotype effects on aging dependent changes in cardiac mitochondrial function, measured as oxygen consumption, under different substrate conditions in a glutamate based protocol. G/M, glutamate malate; ADP, adenosine diphosphate; SUCC, succinate; ROT, Rotenone; FCCP, carbonylcyanide-*p*-trifluoromethoxyphenylhydrazone. * indicates $p<0.05$ vs. baseline value for the phenotype; # indicates $p< 0.05$ vs. previous treatment condition for the phenotype.

Progressive, stepwise increases in oxygen consumption above baseline were seen with the addition of ADP, and with subsequent addition of glutamate and then succinate in the plamitoyl carnitine (fatty acid) protocol. As in the previous protocol, values for oxygen consumption are consistent with those reported in isolated fibers from young rat, and there were no differences between the phenotypes, suggesting that there was no age dependent decrement in cardiac mitochondrial function, and no impact of phenoptype on that outcome. (Table 17, Figure 31).

TABLE 17. Summary of oxygen consumption data under Palmitate/Malate (Fatty Acid) protocol conditions, obtained using cardiac mitochondria isolated from aged HCR and LCR animals.

		Condition					
Group		**Baseline**	**M/PC**	**ADP**	**GLUT**	**SUCC**	**FCCP**
HCR		411.4	580.8	1871.3	2493.3	3036.7	2657.5
		10.7	71.6	615.6	852.8	1099.0	835.2
		96.4	107.6	180.2	249.2	301.5	318.2
	mean	172.9	253.4	889.0	1198.5	1479.1	1270.3
	SEM	121.8	164.1	506.9	670.5	812.1	709.5
			0.2941	0.0145	0.0088	0.0065	0.0082
				0.1074	0.0996	0.0942	0.1088
LCR		437.8	611.2	1019.0	980.1	1381.9	1186.1
		123.9	141.1	483.5	811.2	1036.0	856.1
		134.1	156.4	543.9	837.5	1009.7	936.7
		233.9	287.7	795.1	1058.9	1192.6	1206.4
		59.2	237.3	555.6	954.2	1104.9	994.2
		153.5	198.2	464.7	729.1	879.9	874.7
	mean	190.4	272.0	643.6	895.1	1100.8	1009.0
	SEM	54.5	71.3	89.3	50.1	70.4	62.5
p vs. baseline			0.1588	0.0002	0.0000	0.0000	0.0000
p vs. previous				0.0001	0.0048	0.0021	0.0247
p vs. HCR		0.4521	0.4621	0.3391	0.2587	0.3438	0.3742

Baseline; oxygen consumption with only mitochondria and buffer; **M/P**, oxygen consumption with subsequent addition of malate/palmitoyl carnitine; **ADP**, oxygen consumption with subsequent addition of ADP; **GLUT**, oxygen consumption with subsequent addition of glutamate; SUCC, oxygen consumption with subsequent addition of succinate; **FCCP**, oxygen consumption with subsequent addition of carbonylcyanide-*p*-trifluoromethoxyphenylhydrazone

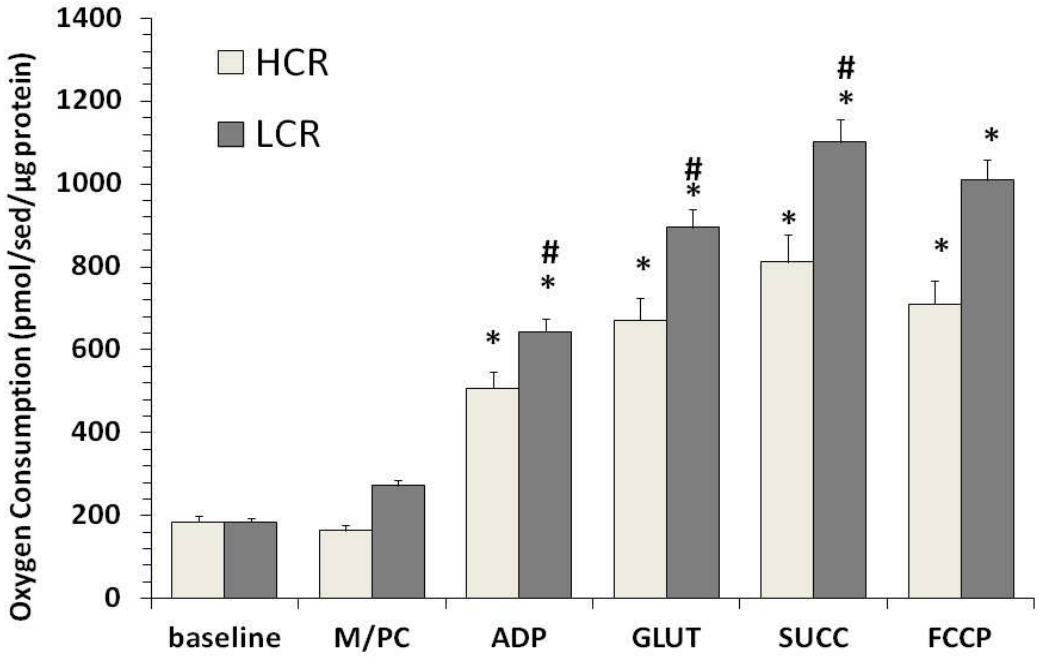

<u>Figure 31.</u> Comparison of phenotype effects on aging dependent changes in cardiac mitochondrial function, measured as oxygen consumption, under different substrate conditions in a fatty acid based protocol. M/PC, malate/ palmitoyl carntiine; ADP, adenosine diphosphate; GLUT, glutamate; SUCC, succinate; FCCP, carbonylcyanide-*p*-trifluoromethoxyphenylhydrazone. * indicates $p<0.05$ vs. baseline value for the Comparison of phenotype effects on aging dependent changes in mitochondrial function is a glucose based protocol. * indicates $p<0.05$ vs. baseline value for the phenotype; # indicates $p< 0.05$ vs. previous treatment condition for the phenotype.

Doxorubicin treatment caused a significant increase in the oxygen consumption of cardiac mitochondria isolated from LCR animals stimulated with glutamate malate, ADP, and succinate, but not in mitochondira isolated from HCR animals (Table 18, Figure 32). In contrast, doxorubicin treatment did not produce phenotype specific differences in mitochondrial oxygen consumption when stimulated with the fatty acid based protocol (Table 19, Figure 33).

When compared to the control responses, doxorubicin increased mitochondrial respiratory capacity 2-5 fold in LCRs in the glutamate protocol, but HCR isolates did not increased respiratory capacity in response Doxorubicin treatment in any substrate protocol (Figures 34 and 35).

The doxorubicin induced increase in respiratory capacity may have been a compensation for a decrease in total mitochondrial number, as mitochondrial protein was approximately 30% higher ($p = 0.061$) in the HCR animals under all conditions tested (Figure 36). Doxorubicin did not cause a decrease in mitochondrial protein content, but the baseline differences between LCRs and HCRs may have required an inducible adaptation in the LCRs at the mitochondrial level to respond to the increased stress placed on the system by doxorubicin treatment.

TABLE 18. Summary of oxygen consumption data under Glucose/Malate protocol conditions, obtained using cardiac mitochondria isolated from aged HCR and LCR animals 10 days after doxorubicin treatment.

	Condition					
Group	**baseline**	**G/M**	**ADP**	**SUCC**	**ROT**	**FCCP**
HCR + Dox	249.9	332.7	658.7	1160.4	744.0	737.6
	339.7	500.1	609.1	901.3	747.1	801.3
	97.7	122.8	527.2	1066.8	574.4	533.1
	125.1	113.2	500.3	874.1	496.2	423.9
	65.1	90.6	362.2	568.5	292.8	267.8
mean	175.5	231.9	531.5	914.2	570.9	552.7
SEM	51.6	80.0	50.9	101.3	84.8	98.5
p vs Baseline		0.0671	0.0002	0.0007	0.0006	0.0011
p vs. Previous			0.0024	0.0018	0.0021	0.2187
LCR + Dox	389.9	519.3	580.2	754.1	665.8	693.9
		223.2	1086.1	1733.3	1227.6	1160.1
	108.5	242.6	1386.6	2796.7	1242.3	1195.7
	80.5	101.6	135.9	234.7	197.7	181.1
	103.0	137.1	342.8	569.6	378.4	389.3
	1030.1	1371.0	3427.9	5695.5	3783.8	3893.1
	2565.4	3017.1	5286.2	7710.9	5296.6	4873.9
	530.1	1777.1	7069.1	9750.5	4527.0	4193.2
mean	686.8	923.6	2414.4	3655.6	2164.9	2072.5
SEM	316.3	371.4	912.3	1280.6	720.2	675.8
p vs Baseline		0.0422	0.0351	0.0213	0.0163	0.0154
p vs. Previous			0.0239	0.0074	0.0239	0.1013
p vs HCR	0.1193	0.0539	0.0390	0.0349	0.0314	0.0299

Baseline; oxygen consumption with only mitochondria and buffer; **G/M**, oxygen consumption with subsequent addition of Glutamate/malate; **ADP**, oxygen consumption with subsequent addition of ADP; **SUCC**, oxygen consumption with subsequent addition of succinate; **ROT**, oxygen consumption with subsequent addition of Rotenone; **FCCP**, oxygen consumption with subsequent addition of carbonylcyanide-*p*-trifluoromethoxyphenylhydrazone

TABLE 19. Summary of oxygen consumption data under Palmitate/Malate (Fatty Acid) protocol conditions, obtained using cardiac mitochondria isolated from aged HCR and LCR animals 10 days after doxorubicin treatment.

		Condition					
Group		**Baseline**	**M/PC**	**ADP**	**GLUT**	**SUCC**	**FCCP**
HCR + DOX		227.9	323.4	870.2	1326.6	1632.8	1282.7
		403.3	561.4	987.9	978.5	1350.9	1169.2
		99.5	155.9	768.5	1158.4	1437.3	1014.9
		114.5	124.2	514.8	994.4	1287.6	1009.9
		340.0	340.0	340.0	340.0	340.0	340.0
	mean	237.0	301.0	696.3	959.6	1209.7	963.3
	SEM	60.1	78.1	118.4	167.3	225.1	164.0
p vs. baseline			0.0465	0.0104	0.0118	0.0095	0.0089
p vs. previous				0.0104	0.0378	0.0090	0.0142
LCR + DOX		435.6	594.4	817.4	903.5	1040.1	981.3
		9.3	304.1	1865.5	2579.6	3172.2	1809.1
		94.9	316.1	399.6	1481.1	2808.9	1487.0
		108.0	101.6	183.5	235.2	287.6	295.9
		146.4	178.0	591.6	919.9	1130.6	837.8
		283.6	344.9	654.1	901.7	1104.0	1040.7
		51.7	208.8	746.5	1229.9	1387.0	1235.1
		150.5	166.3	289.4	354.5	428.1	422.0
	mean	160.0	276.8	693.4	1075.7	1419.8	1013.6
	SEM	48.7	54.3	184.8	259.1	368.3	179.5
p vs. baseline			0.0092	0.0162	0.0071	0.0073	0.0018
p vs. previous				0.0236	0.0104	0.0294	0.0453
p vs. HCR		0.1730	0.4029	0.4950	0.3570	0.3181	0.4201

Baseline; oxygen consumption with only mitochondria and buffer; **M/P**, oxygen consumption with subsequent addition of malate/palmitoyl carnitine; **ADP**, oxygen consumption with subsequent addition of ADP; **GLUT**, oxygen consumption with subsequent addition of glutamate; SUCC, oxygen consumption with subsequent addition of succinate; **FCCP**, oxygen consumption with subsequent addition of carbonylcyanide-*p*-trifluoromethoxyphenylhydrazone

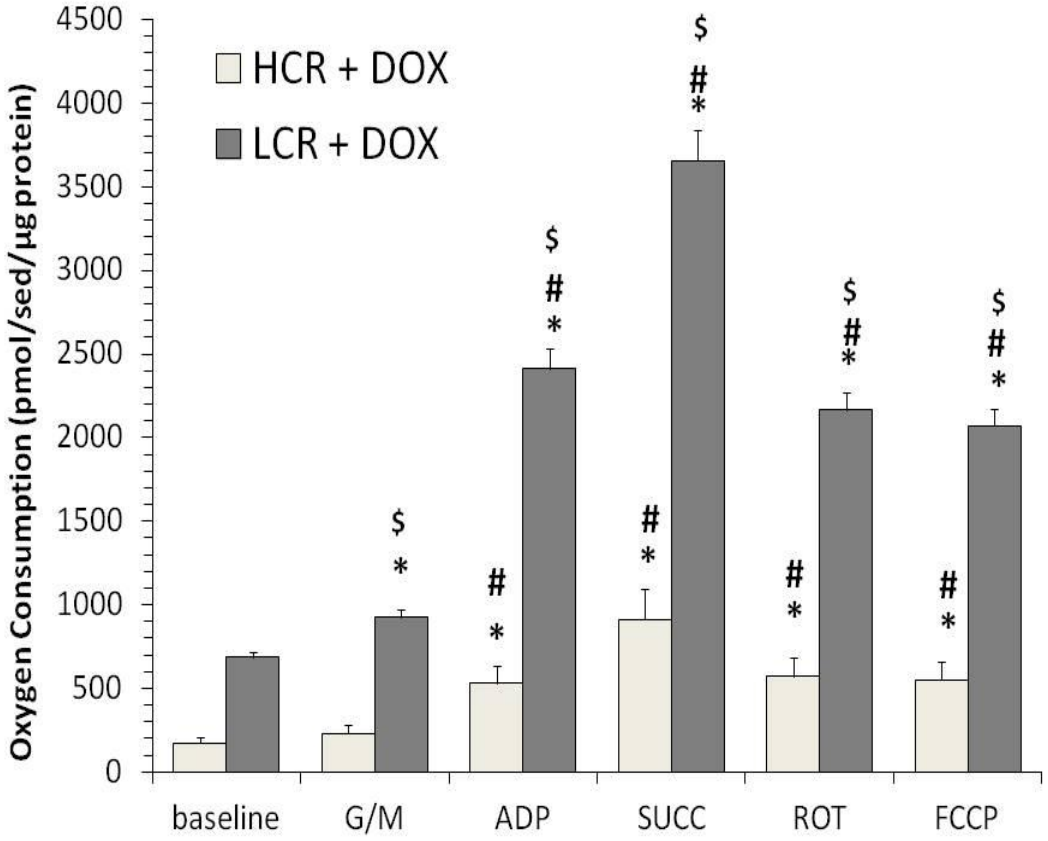

Figure 32. Comparison of phenotype influence on doxorubicin dependent changes in cardiac mitochondrial function, measured as oxygen consumption, under different substrate conditions in a glutamate based protocol. G/M, glutamate malate; ADP, adenosine diphosphate; SUCC, succinate; ROT, Rotenone; FCCP, carbonylcyanide-*p*-trifluoromethoxyphenylhydrazone . * indicates $p<0.05$ vs. baseline value for the phenotype; # indicates $p< 0.05$ vs. previous treatment condition for the phenotype; $ indicates $p<0.05$ vs. HCR value under the same conditions.

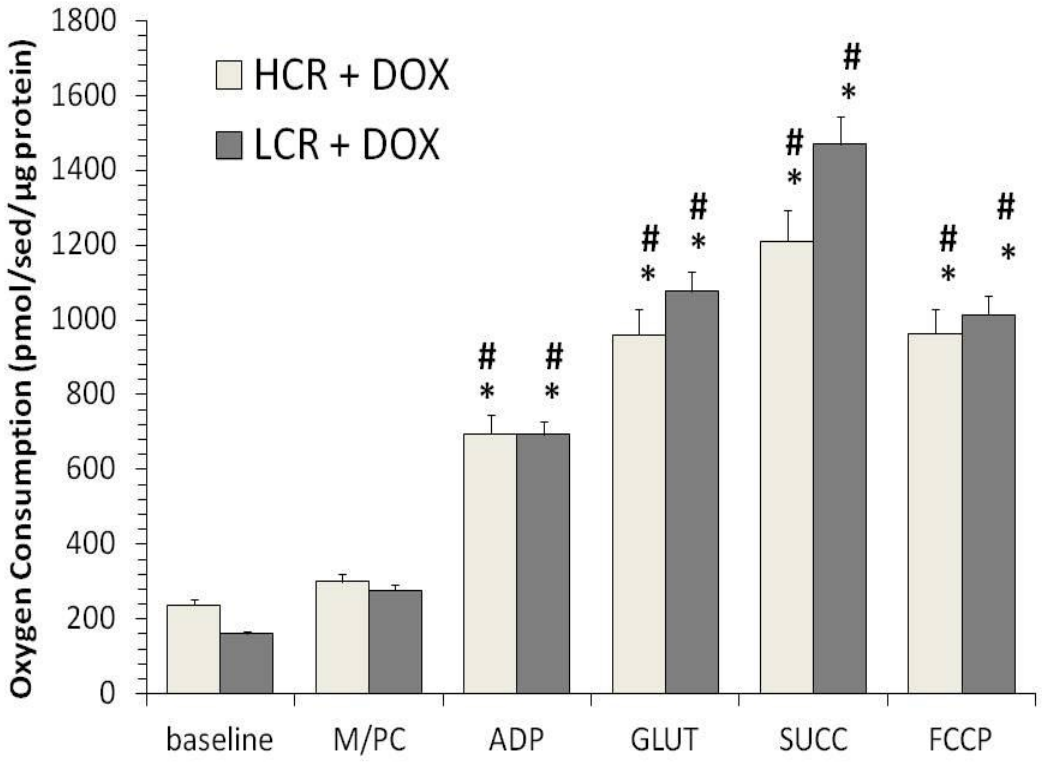

<u>Figure 33.</u> Comparison of phenotype influence on doxorubicin dependent changes in cardiac mitochondrial function, measured as oxygen consumption, under different substrate conditions in a fatty acid based protocol. M/PC, malate/ palmitoyl carntiine; ADP, adenosine diphosphate; GLUT, glutamate; SUCC, succinate; FCCP, carbonylcyanide-*p*-trifluoromethoxyphenylhydrazone. * indicates $p<0.05$ vs. baseline value for the Comparison of phenotype effects on aging dependent changes in mitochondrial function is a glucose based protocol. * indicates $p<0.05$ vs. baseline value for the phenotype; # indicates $p< 0.05$ vs. previous treatment condition for the phenotype.

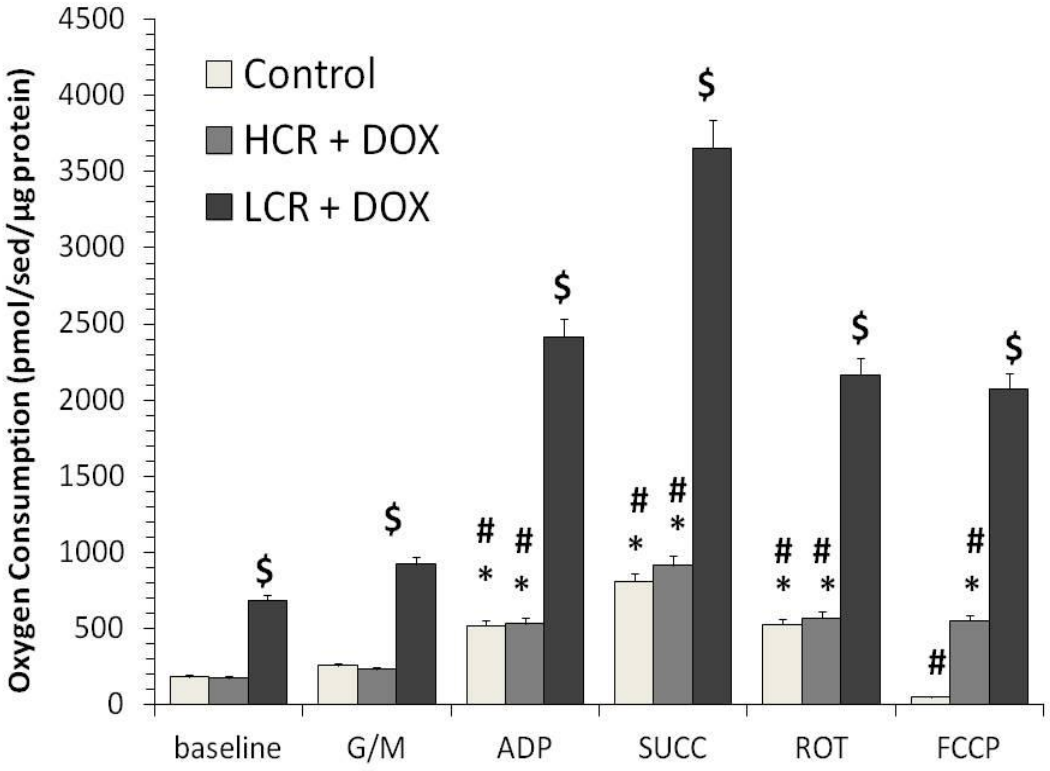

Figure 34. Comparison of doxorubicin effects on cardiac mitochondrial function, measured as oxygen consumption, under different substrate conditions in a glutamate based protocol. G/M, glutamate malate; ADP, adenosine diphosphate; SUCC, succinate; ROT, Rotenone; FCCP,. carbonylcyanide-*p*-trifluoromethoxyphenylhydrazone * indicates $p<0.05$ vs. baseline value for the phenotype; # indicates $p< 0.05$ vs. previous treatment condition for the phenotype; $ indicates $p<0.05$ vs. HCR value under the same conditions.

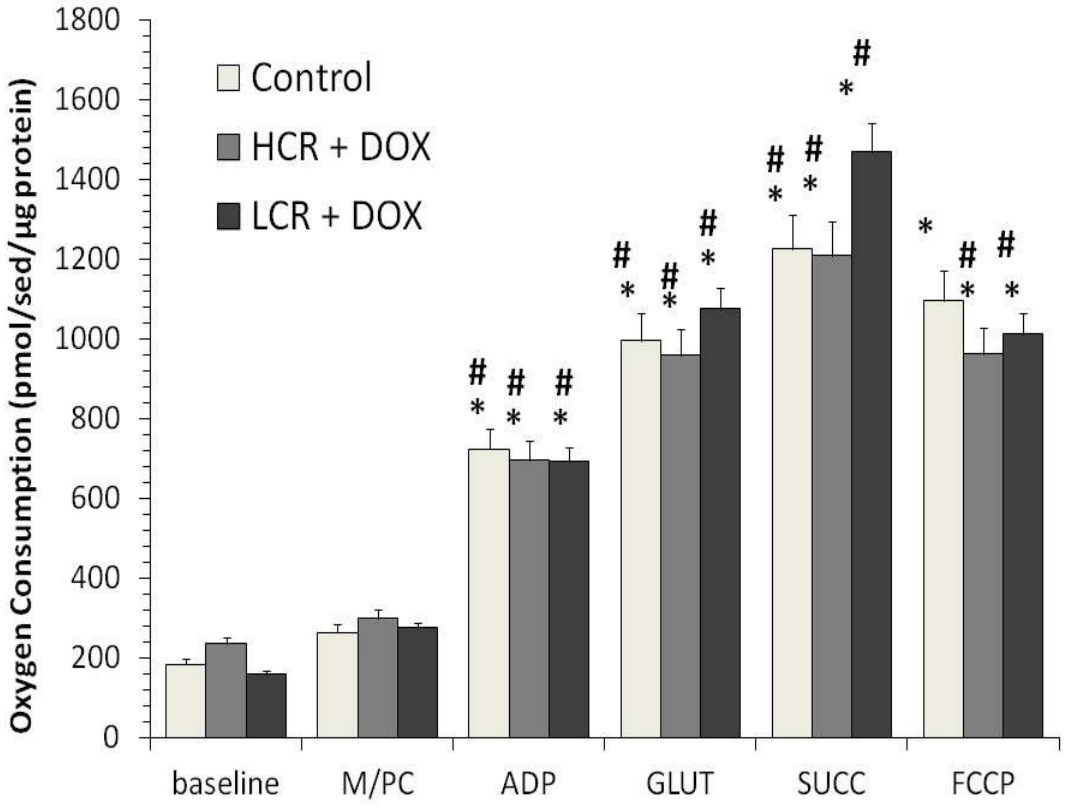

<u>Figure 35.</u> Comparison of doxorubicin effects on cardiac mitochondrial function, measured as oxygen consumption, under different substrate conditions in a fatty acid based protocol. M/PC, malate/ palmitoyl carntiine; ADP, adenosine diphosphate; GLUT, glutamate; SUCC, succinate; FCCP, carbonylcyanide-*p*-trifluoromethoxyphenylhydrazone . * indicates $p<0.05$ vs. baseline value for the Comparison of phenotype effects on aging dependent changes in mitochondrial function is a glucose based protocol. * indicates $p<0.05$ vs. baseline value for the phenotype; # indicates $p< 0.05$ vs. previous treatment condition for the phenotype.

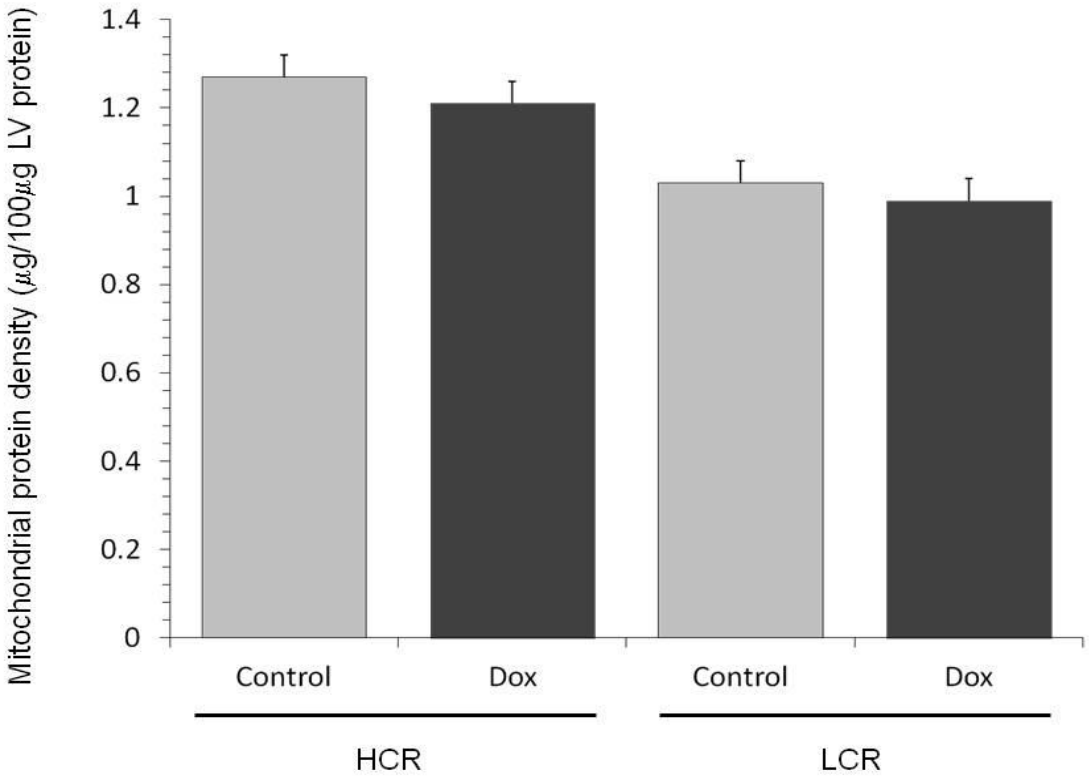

Figure 36. Comparison of mitochondrial protein amounts in control and doxorubicin treated animals. Doxorubicin did not cause a loss in mitochondrial protein in either phenotype, but HCRs consistently demonstrated 30-35% higher mitochondrial protein content per unit LV mass than the LCRs.

CHAPTER IV: DISCUSSION

Aerobic exercise capacity influences quality of life and has been shown to be powerful predictor of mortality (Koch et al., 2008). The protective effects of active aerobic capacity, as studied through exercise preconditioning training, have been well described as improving myocardial tolerance to harmful oxidative stress (Ascensao et al., 2012). However, the role of innate aerobic capacity, versus active exercise training, is largely unexplored. Therefore, the goal of this study was to examine the effect of inherent differences in aerobic capacity in response to Doxorubicin-induced toxicity. As HCRs demonstrate lower cardiovascular risk factors, we wanted to test specifically whether HCRs were less susceptible to doxorubicin-induced cardiotoxicity (Lujan et al. 2006). Our hypothesis was that the low aerobic running capacity (LCR) phenotype will show increased susceptibility to the DOX-induced cardiotoxicity when compared to the high aerobic running capacity (HCR) phenotype. In this study, it was hypothesized that impairment of mitochondrial function and cardiac performance may link reduced fitness from doxorubicin-induced cardiotoxicity. The results indicate that our hypothesis was oversimplified, as the mitochondrial function and cardiac performance responses to Doxorubicin varied with the divergent phenotypes.

In order to focus on the role of cardiac dysfunction after doxorubicin treatment in aging aerobic capacity phenotypes, we studied two strains of rat presenting the divergent phenotypes: the HCR and LCR rats. The control animals that were not treated with doxorubicin did not perform significantly different in either test, suggesting that aging reduced the phenotypic differences seen in younger animal studies. We expected that the HCR rats would outperform the LCR animals, which corresponds with other rat strain studies,

in which the rats with the longest life spans are less affected by age-related pathology and show completely normal mitochondrial function in the elderly (Lemieux et al., 2010). Interestingly, possibly due to a husbandry effect, our LCR animals outlived the HCR animals when considering spontaneous mortality. However, given insignificant differences between our control animal phenotypes in mitochondrial function and cardiac performance, it is difficult to dispel any of the uncertainty in the role that aging plays in attenuating the intrinsic benefits of a high aerobic capacity. This suggests that as one ages, the benefit of an innate high aerobic capacity may reduce with age. A possible explanation to the demise of this benefit is that oxidative damage to the mitochondrial DNA and electron transport chain accumulates with age. This reduces mitochondrial energetic capacity, further stimulating oxygen free radical production. The resulting mitochondrial DNA damage inhibits mitochondrial biogenesis and increases replication errors and mitochondrial DNA deletions, thus creating a vicious circle. Doxorubicin treatment in conjunction with an aged phenotype is therefore an ideal situation for these events to occur, as oxygen free radicals are produced and mitochondrial DNA deletion takes place. Cardiac failure as a result of Dox administration is attributed to increased reactive oxygen species (ROS) production by the mitochondria. Specifically, it has been proposed that Dox stimulates ROS through mitochondrial NADH dehydrogenase, leading to the generation of a free radical cascade with a potent oxidizing potential. However, one study reported lower oxidative DNA mutations despite greater reactive oxygen species in skeletal muscles from HCR rats (Tweedie et al, 2011). Therefore, the phenotypic benefit of a high aerobic capacity may have disappeared due to an altered

mitochondrial biogenesis from the preexisting excessive amounts of oxidative damage due to aging (Alexeyev et al., 2004; Alexeyev et al., 2009).

Furthermore, it is expected that if the dosage and consequently, the concentration of the doxorubicin was higher, the inhibition of both fatty acids and glucose oxidation would have been seen (Abdel-aleem et al., 1997). Following doxorubicin treatment, the LCR animals exhibited elevated levels of mitochondrial respiration, especially in the glutamate-based protocol. Also, the LCR animals responded by increasing their cardiac volumes but did not succeed in increasing their cardiac output, while the HCRs increased their heart rate and cardiac output, albeit in the total absence of exercise training. Taken together, these data demonstrate that intrinsic aerobic capacity influences the adaptive responses following DOX-injury and perhaps the progression of DOX-induced cardiotoxicity.

Similarly to the effects of endurance exercise, the possibility exists that HCRs have improvements in innate myocardial antioxidant capacity which contribute protection against the doxorubicin-induced damage (Quindry et al., 2005). Inversely, LCR rat hearts may be vulnerable to doxorubicin cardiotoxicity due to limited antioxidant mechanisms that could protect them from oxidative stress (Ashour et al., 2012). However, antioxidants are not cardiac specific and therefore reduce oxidative stress nonspecifically (Oliveira et al., 2011). Thus, the results from the present investigation provide novel insight into potential mechanisms associated with cardiovascular failure in a system that allows for each strain to serve as a control for unknown environmental changes (Rivas et al., 2011).

As one ages, mitochondrial mutations accumulate causing mitochondrial dysfunction and a decline in antioxidant capacity, which correlate with aerobic capacity. A mitochondrial

defect associated with aging has involved a decrease in complex III and IV activities (Fannin et al., 1999; Moghaddas et al., 2002; Lesnefsky et al., 2006).The addition of the doxorubicin stress may accelerate these mutational processes and advance the decline of normal physiological functions. Moreover, there is a greater necessity of cardiac tissue to avoid mutational insult as cardiomyocytes are postreplicative and unable to repair the DNA damage. The progressive accumulation of mitochondrial mutations in affected hearts will increase the severity of the organ phenotype damage associated with those mutations (Stevenson et al., 2006). This lack of regeneration capability in conjunction with cardiomyocyte damage could explain the deterioration of cardiac function (L'Ecuyer et al., 2006). Reactive oxygen species cause injury to mitochondrial transcription that exacerbates mitochondrial dysfunction by inhibiting synthesis of respiratory chain proteins (Tang et al., 2002). The proximity of the ETC to the relatively unprotected mitochondrial DNA makes mitochondrial transcription proteins particularly vulnerable to oxidative stress (Kristal et al., 1994). Complex I is the largest ETS complex and seven of its 40 constituent proteins are encoded by mitochondrial DNA whereas all 4 proteins of Complex II are encoded strictly by nuclear DNA. Thus, one hypothesis to explain the decreased activity of Complex I could be due to oxidative damage of mitochondrial DNA (Tang et al., 2002). Damaged mitochondria due to oxidative stress are a serious hazard to cardiac health and performance.

Cardiac efficiency is the ratio between energy output (work) and energy input (myocardial oxygen consumption) for the heart. An increase in cardiac work is consistent with more efficient oxygen utilization by the heart to produce ATP and in turn, mechanical work (McCormack et al., 1998). The evaluation of mitochondrial function is critical to

explore how doxorubicin affects cardiac performance as the organelle supplies cardiomyocytes with ATP, a crucial energy source for muscle contraction. Doxorubicin has been shown to cause a significant decrease in ATP (Ashour et al., 2012). Thus, a depressed mitochondrial function leads to a reduced work capacity, which is demonstrated as a lowered cardiac performance as evident through cardiac output. For this reason, we investigated the mitochondrial respiration properties of cardiac mitochondria from the LCR/HCR animals.

Our study identifies change in mitochondrial function with doxorubicin treatment in isolated cardiac mitochondria that varies between the rat strains. Measurements of oxygen consumption provide an appropriate indication of mitochondrial function. Respirometry studies were performed to determine inefficient cardiac mitochondrial function, which is known to lead to added oxidant stress levels and may therefore play a direct role in the reduction of cardiac performance (Stevenson et al., 2006). The addition of different substrates and analysis of electron flow from the complexes of the ETC is used to determine the functional activity of the ETC and allows for the identification of a specific impaired complex. In the glutamate-based protocol, the sequential injections of glutamate and malate were used to determine the effect of these substrates on mitochondrial respiration when electrons are provided to complex I. A further injection of succinate was used to assess the effect of electron input through complex I and complex II. Rotenone was added to specifically inhibit complex I, thereby allowing the evaluation of mitochondrial respiration through only complex II. The analysis of beta-oxidation metabolism substrates were analyzed using the palmitoyl-carnitine based respiration protocol. In muscles, mitochondrial fatty acid

beta-oxidation provides acetyl-CoA into the Krebs cycle for production of ATP. When supported with beta-oxidation, there was not a significant difference in the response, but generally DOX-treated HCR rats exhibited depressed oxygen consumption levels and the LCRs increased in oxygen consumption.

There are several explanations for the differences exhibited in the LCR and HCR responses to Doxorubicin treatment. The first explanation is that because of their genetic endowment, the HCR rats have less need to adapt to the doxorubicin injury than the LCR rats. The HCRs may have been intrinsically prepared to handle the doxorubicin insult. Thus, the lack of a mitochondrial respiration response by the HCR animals to the drug may be because the stress was not as impactful for that phenotype in comparison to the LCRs. Supporting evidence for such a postulate can be seen in our oxygen consumption data; the LCR rats increased their oxygen consumption after doxorubicin treatment while the HCR rats exhibited relatively stable rates. Moreover, after doxorubicin treatment, the HCRs responded by increasing their heart rate, while the LCRs increased their volumes. This supports the explanation that this same experimental drug treatment induced a different injury within the phenotypes due to the genetic endowment. Although both phenotypes were given similar dosages, it is likely that the HCRs are endowed with inherent advantages that make them better equipped to tolerate the doxorubicin cardiac insult and therefore did not need to recover like the LCRs. One innate advantage of the HCRS may be a higher mitochondrial density.

As previously reported, doxorubicin is associated with several signs of cardiomyopathy: LV hypertrophy, changes in ventricle diameter, cardiomyocytes

hypertrophy and loss, fibrosis and collagen deposition (Lemieux et al., 2010; Schwartz et al., 1998). These findings are consistent with our observation that DOX-treated LCR hearts have increased geometric dimensions and stroke volume, but a depressed cardiac output, which may reflect a compensatory remodeling response to the doxorubicin toxicity in the heart. The correspondence between DOX-treated LCRs and models of cardiomyopathy is testament to the importance of low aerobic capacity in the development of cardiac failure. Our investigation supports the thesis that in aged populations, depressed aerobic capacity is the antecedent of cardiac dysfunction.

Other characteristics of the animal model may have played a role in the divergent response to Doxorubicin. The LCR animals' characteristic large adiposity could have been a factor in doxorubicin's cardiotoxicity as it is recognized that the drug does not achieve high concentrations in fat tissue and that obesity has been shown to slow the metabolism of the drug. Therefore, it is hypothesized that since anthracyclines do not distribute into fat then equivalent doses based on body surface area may lead to higher concentrations of doxorubicin in the hearts of LCRs than HCRs (Silber et al., 1993). Moreover, it is well studied that LCR rats become exhausted more quickly, run for shorter distances and at slower paces compared to HCR rats (Buck et al., 2012). Interestingly, it has also been found that there is a sex effect with females having higher numbers of functional mitochondria than males (Demarco et al., 2012). HCR rats have been shown to have higher markers of mitochondrial content in their locomotor muscles (Tweedie et al., 2011). HCRs have been found to have superior mitochondrial content in skeletal muscle. Increased body weight, decreased fatty acid oxidation, and reduced insulin sensitivity has been associated with the reduced

mitochondrial content in the skeletal muscle of LCR rats (Rivas et al., 2011). A determinant of aerobic capacity performance is local oxidative capacity, namely, mitochondrial density. To achieve a given rate of oxygen uptake, greater mitochondrial density will require a lesser degree of activation per mitochondrion. Subsequently, smaller increases in controllers of respiration, such as ADP (Walsh et al., 2006). Due of these inherent advantages, it is likely that doxorubicin produced less insult in the HCR rats than the LCRs, and consequently induced less observable changes in mitochondrial respiration. Taken together, there is a strong argument that the differences between the phenotypes in their adaptive responses to doxorubicin is determined by the inherent differences that exist due to the genetic endowment.

A second possible explanation for the differences in response to DOX between the phenotypes is that the two groups adapt similarly, but the LCR response is attenuated due to poor intrinsic aerobic capacity. In the cardiac performance data, we see that the LCR animals' cardiac output is initially decreased, but by the fourteenth day, the LCRs demonstrated increases in this value to similar levels as the HCRs. These data support the explanation that the adaptive responses employed by the HCR and LCR animals are similar but the timing of the response is the component that is influenced by inherent aerobic exercise capacity. However, one item to take into consideration is that the dosage of doxorubicin may be affecting the animals in a bimodal manner. It is possible that the dosage of doxorubicin may have caused a two-waved systemic response, and a larger dosage may have produced a more direct cardiotoxic effect. Therefore, the change in our cardiac performance responses throughout the 10 day study could be separated into the first initiatory stage where local

reactions were activated, and days later, a secondary release of effects may have been induced. This secondary wave may be responsible for the wide range of systemic effects (Ceciliani et al., 2002). Many factors are involved in the initiation and progression of doxorubicin cardiotoxicity and the finding that the drug response may be bimodal is an important technical consideration for anyone involved in the studies in this model, in particular with regard to the interpretation of findings (Wapstra, et al., 1999).

Though our specific doxorubicin dose has been extensively used as a treatment in rats, it is likely that different doses of doxorubicin induce effects that vary considerably among investigators. Under the experimental conditions of our laboratory, in the aged rat strains, our single intraperitoneal 7.5mg/kg doxorubicin dose appeared to be the most appropriate dose. However, our study results may have also varied if we sacrificed the animals earlier (such as day 4 or day 7) and examined mitochondrial function sooner. We may have seen a more pronounced difference in the cardiac mitochondrial function between the phenotypes. Based on our results, we most likely examined acute doxorubicin cardiotoxicity, which are nonlifethreatening events that are resolved within a week. Acute cardiotoxicity damage resolves promptly to the cessation of doxorubicin infusion and rarely precludes further continuation of treatment. However, the types of chronic toxicity are irreversible and clinically significant, substantially affecting overall morbidity and mortality and requiring long-term therapy (Dazzi, et al., 2001). Studies have shown that the genetic makeup of patients may modulate the individual risk to develop cardiotoxicity (Deng et al., 2007; Wojnowski et al., 2005). Thus, in experimental toxicity induced by doxorubicin, the dose of DOX used is crucial as it appears to be an important determinant not only of the

severity of the cardiotoxicity that eventually ensues, but notably of the responsiveness of the HCR and LCR animals.

A third possible explanation is that the animal phenotypes utilize different mechanisms to adapt to the doxorubicin treatment. This conclusion is supported by the cardiac performance results that show that the HCR rats changed heart rate but the LCR rats did not. Furthermore, the LCR phenotype adapted to DOX by increasing the volumes, but the HCR rats did not demonstrate this change. These data support the explanation that difference in adaptive response to doxorubicin may be due to different mechanism and pathways. We also showed that doxorubicin induced an adaptation of the mitochondria in LCRs whereby the glutamate-based oxygen consumption increased. As discussed earlier, if the doxorubicin dose is mild, a low aerobic capacity phenotype induces an adaptive mitochondrial respiration and increased volumes. The HCR animals did not exhibit a change in mitochondrial respiration but doxorubicin did induce an elevated heart rate which transpired into an increased cardiac output. In contrast, it is theorized that a more severe dosage results in an accumulation of doxorubicin in mitochondria that subsequently leads to heart failure. Thus, these results suggest that the beneficial effects of a high aerobic capacity phenotype encompass unique protective mechanisms to cardiotoxicity, guiding to an improved mitochondrial and cardiac function, and thereby, to a higher fitness. Hence, intrinsic aerobic capacity may respond to the same stressor with different mechanistic adaptive responses determined in part by the same gene profiles that establish intrinsic aerobic running capacity.

The present study has established that intrinsic aerobic capacity influences adaptive cardiac responses to doxorubicin insult. The high intrinsic aerobic capacity phenotype responds by increasing heart rate and cardiac output within ten days. However, this phenotype makes no significant changes in mitochondrial respiration. Therefore, it may be suggested that this phenotype utilizes a tachycardiac response to the doxorubicin treatment. This increase in cardiac output may be possible due to the HCR animals 25% greater amount of mitochondrial density.

In conclusion, this study provides new insight into the effects of doxorubicin treatment on mitochondrial and cardiac function in rats with divergent aerobic capacities. Our investigation demonstrates that selection for the trait of low intrinsic aerobic capacity diminishes the performance of cardiac muscle in response to doxorubicin treatment. After drug infusion, the impaired cardiac output in animals bred for inferior aerobic capacity was associated with elevated cardiac volume dimensions and elevated mitochondrial respiration, particularly in the glutamate-based protocol. Furthermore, selection for high aerobic capacity, in the absence of exercise training, endows increased mitochondrial density, heart rate and cardiac output after doxorubicin treatment. These data provide some novel evidence that differences in the mitochondrial function and cardiac performance may have a role in the divergence in aerobic capacity in the LCR/HCR model. This is in agreement with previous studies that have reported data suggesting that reduced mitochondrial function may be an inherited defect and leads to the progression of metabolic disease states and aging (Rivas et al., 2011).

There are abundant opportunities in the future to study doxorubicin, particularly because it is one of the most widely prescribed chemotherapeutic agents while the mechanism of action is largely unknown. Although a number of mechanisms have been postulated to explain the pathogenesis of cardiotoxicity and its associated clinical manifestations, the precise details of the cellular and subcellular alterations remain to be elucidated. Because no single mechanism that could fully explain the development of the depressed cardiac/mitochondrial function has been identified, it is likely that the cause is multifactorial. In this regard, there has been a recent surge in experimental studies suggesting mitochondria may be intimately involved in the cardiotoxicity. Further investigation of whether there are differences in markers of cardiac mitochondrial capacity and density between phenotypes should be determined. Methods to verify mitochondrial content include analyzing maximal citrate synthase activity, expression of mitochondrial proteins through western blotting and quantifying by transmission electron microscopy. Potential future projects based on the insight gained from the current study should include direct measurements of oxidative stress using a GSH/GSSG assay or spectrofluorometric determination of hydrogen peroxide. Also, it has been suggested that differences in individual antioxidant defenses may hold the key to understanding doxorubicin susceptibility, but no studies have demonstrated a clear link or plausible mechanism for this deficiency. Therefore, those with high aerobic capacity are expected to have greater antioxidant defenses to deal with stresses, such as doxorubicin treatment (Stevenson et al., 2006). More research needs to explore the impact that intrinsic aerobic capacity has on the

role of doxorubicin and investigate effective agents that block the detrimental cardiotoxic effects of doxorubicin while preserving antitumor activity.

According to the American Cancer Society and the National Cancer Institute, the number of Americans living with cancer is estimated to increase by nearly a third to almost 18 million by 2022 (Siegel et al., 2012). Of the cancer survivor populations, there are approximately 350,000 pediatric cancer survivors currently in the United States (Mariotto et al., 2009). As the trend of improved survival and population aging converge to produce an increasing group of cancer survivors, it is becoming more vital that patients not only survive through cancer therapies, but also live beyond their cancer treatment. The fact that the more potent the anticancer agents, the greater the toxicity to normal tissues leads to the use of only a fraction of the curable dose of a drug. This is especially true for the anticancer agent doxorubicin, which has notorious cardiotoxic effects. Therefore, it is vital that advances to effectively protect against doxorubicin's cardiotoxicity are developed to prevent cancer survivors from forming chronic life-threatening conditions, such as heart failure secondary to this therapy.

References

Abdel-aleem, S., El-Merzabani, M.M., Sayed-Ahmed, M., Taylor, D.A. & Lowe, J.E. (1997). Acute and chronic effects of Adriamycin on fatty acid oxidation in isolated cardiac myocytes. *J Mol Cell Cardiol 29*, 789-797.

Ago, T., Matsushima, S., Kuoda, J. & Sadoshima, J. (2010). The NADPH oxidase Nox4 and aging in the heart. *Aging 2*(12), 12-16.

Alexeyev, M.F., LeDoux, S.P. & Wilson, G.L. (2004). Mitochondrial DNA and aging. *Clin Aging 107*, 335-364.

Alexeyev, M.F. (2009). Is there more to aging than mitochondrial DNA and reactive oxygen species? *Febs J 276* (20). 5768-87.

Anderson, E.J., Katunga, L.A. & Willis, M.S. (2011) Mitochondria as a source and target of lipid peroxidation in healthy and diseased heart. *CEPP 39*, 179-193.

Anderson, E.J., Kypson, A.P., Rodriguez, E., Anderson, C.A., Lehr, E.J. & Neufer, P.D. (2009) Substrate-specific derangements in mitochondrial metabolism and redox balance in the atrium of type 2 diabetic human heart. *J Am Coll Cardiol 54*(20): 1891-1898.

Anderson, E.J., Lustig, M.E., Boyle, K.E. (2009). Mitochondrial H2O2 emission and cellular redox state link excess fat intake to insulin resistance in both rodents and humans. *J Clin Invest 119*, 573-581.

Arai, M., Yoguchi, A., & Takizawa, T. (2000). Mechanism of doxorubicin-induced inhibition of sarcoplasmic reticulum Ca(2+)-ATPase gene transcription. *Circ Res*, *86,* 8-14.

Arcamone, F., Animati, F., Berettoni, M, Bigioni, M & Cipollone A. (1997). Doxorubicin disaccharide analogue: Apoptosis-related improvement of efficacy *in vivo*. *J Natl Cancer Inst*, *89*(16), 1217-1223.

Armstrong, L., Balady, G., Berry, M. & Wallace J. (2006). ACSM's guidelines for exercise testing and prescription. 7th ed. Philadelphia, PA: Lippincott Williams & Wilkins; 133-173.

Arola, O.J., Saraste, A., Pulkki, K., Kallajoki M., & Parvinen M. (2000). Acute doxorubicin cardiotoxicity involves cardiomyocyte apoptosis. *Cancer Res, 60,* 1789-1792.

Ascensao, A., Magalhaes J., Soares, J.M.C. & Duarte, J.A. (2005). Moderate endurance training prevents doxorubicin-induced in vivo mitochondriopathy and reduces the development of cardiac apoptosis. *AJP Heart 289*(2), H722-H731.

Ashour, A.E., Sayed-Ahmed, M.M., Abd-Allah, A.R., Korashy, H.M., MAayah, Z.H. & Alhaider, A. (2012). Metformin rescues the myocardium from doxorubicin-induced energy starvation and mitochondrial damage in rats. *Oxid Med Cell Long 2012.*

Balaban, R.S., Nemoto, S. & Finkel T. (2010). Mitochondria, oxidants, and aging. *Cell 120*(4), 483-495.

Berthiaume, J.M. & Wallace, K.B. (2007). Adriamycin-induced oxidative mitochondrial cardiotoxicity. *Cell Biol Toxicol 23*, 15-25.

Billingham, M.E., Mason, J.W., Bristow, M.R., & Daniels, J.R. (1978). Anthracycline cardiomyopathy monitored by morphologic changes. *Cancer Treat Rep, 62,* 865-872.

Boehm, E.A., Jones, B.E., Radda, G.K, Veech, R.L. & Clarke K. (2001). Increased uncoupling proteins and decreased efficiency in palmitate-perfused hyperthyroid rat heart. *AJP-Heart, 280* (3), 977-983.

Bouchard, C. (2012). Genomic predictors of trainability. *Exp Phys 97*(3), 347-352.

Bouchard, C., An, P., Rice, T., & Rao, D.C. (1999). Familial aggregation of VO_{2max} response to exercise training: results from the HERITAGE Family Study. *J App Phys 87*(3), 1003-1008.

Boyle, K.E., Zheng, D., Anderson, E.J., Neufer, P.D., Houmard, J.A. (2011). Mitochondrial lipid oxidation is impaired in cultured myotubes from obese humans. *Int J Obes*.

Bristow, M.R., Billingham, M.E., Mason, J.W. & Daniels, J.R. (1978). Clinical spectrum of anthracyclines antibiotic cardiotoxicity. *Cancer Treat Rep, 62*(6), 873-879.

Britton, S. L. (2005). Animal models of complex diseases: an initial strategy. *IUBMB Life, 57*(3), 631-638.

Buck, B.J., Nolen, L.K., Koch, L.G., Britton, S.L. & Kerman, I.A. Alterations in the brainstem preautonomic circuitry may contribute to hypertension associated with metabolic syndrome. Cardiovascular Risk Factors, Ed. Gasparyan, A.Y., InTech, 2012.

Burniston, J.G., Kenyani, J., Wastling, J.M., Burant, C.F., Koch, L.G. & Britton, S.L. (2011). Proteomic analysis reveals perturbed energy metabolism and elevated oxidative stress in hearts of rats with inborn low aerobic capacity. *Proteomics 11,* 3369-3379.

Cadenas, E. & Davies, K.J.A. (2000). Mitochondrial free radical generation, oxidative stress, and aging. *Free Rad Biol Med 29*(3), 222-230.

Cecarini, V., Gee, J., & Keller J.N. (2007). Protein oxidation and cellular homeostasis: emphasis on metabolism. *ACTA BIOCH BIOPH SIN 1773,* 97-104.

Ceciliani, F., Giordano, A & Spagnolo, V. (2002). The systemic reaction during inflammation: the acute-phase proteins. *PROTEIN PEPT LET 9*(3), 211-223.

Chandran K., Aggarwal, D., Migrino R.Q. & Kalynanaraman B. (2009). Doxorubicin inactivates myocardial cytochrome c oxidase in rats: cardioprotection by Mito-Q. *Biophy J 96,* 1388-1398.

Conklin, K.A. (2005). Coenzyme Q10 for prevention of anthracyclines-induced cardiotoxicity. *Integr Cancer Ther 4*¸110-130.

Dazzi, H., Kaufmann, K. & Follath, F. (2001). Anthracycline-induced acute cardiotoxicity in adults treated for leukaemi. *Ann Oncol 12(*7), 963-966.

Deng, S., Kulle, B., & Hosseini M. (2007). Dystrophin-deficiency increases the susceptibility to doxorubicin-induced cardiotoxicity. *Eur J Heart Fail, 9,* 986-994.

DeMarco, V.G., Johnson, M.S., Ma, L., Pulaka, L., Britton, S.L., Koch, L.G., & Sowers, J.R. (2012). Overweight female rats selectively breed for low aerobic capacity exhibit increased myocardial fibrosis and diastolic function. *Am J Physiol Heart Circ Physiol, in press*.

De Los Santos, J.F. & Buchholz, T.A. (2000). Carcinoma of the male breast. *Curr Treat Options Oncol, 1*, 221-227.

Doroshow, J.H. & Davies, K.J. (1986). Redox cycling of anthracyclines by cardiac mitochondria. II. Formation of superoxide anion, hydrogen peroxide, and hydroxyl radical. *J Biol Chem 261,* 3068-3074.

Ershler, W.B. (2003). Cancer: a disease of the elderly. *J Support Oncol, 1,* 5-10.

Esmat, A.Y., Said, M.M. & Khalil, S.A. In vivo and in vitro studies on the antioxidant activity of aloin compared to doxorubicin in rats. *Drug Devel Res 73,* 154-165.

Felker, G.M., Thompson, R.E., Hare, J.M., & Hruban R.H. (2000). Underlying causes and long-term survival in patients with initially unexplained cardiomyopathy. *N Engl J Med, 342,* 1077-1084.

Ferrans, V.J., Clark, J.R., Zhang, J., & Yu, Z.X. (1997). Pathogenesis and prevention of doxorubicin cardiomyopathy. *Tsitologiia, 39,* 928-937.

Ferrari, Roberto. (1996). The role of mitochondria in ischemic heart disease. *J Cardio Pharm, 2,* 1-10.

Fitts, R.H. (1994). Cellular mechanisms of muscular fatigue. *Phys Rev 74*(1), 49-94.

Frasier, C.R., Moore, R.L., & Brown, D.A. (2011). Exercise-induced cardiac preconditioning: how exercise protects your achy-breaky heart. *J appl Physiol 111*, 905-915.

Gilliam, L.A.A., Moylan, J.S. & Reid, M.B. (2012). Doxorubicin acts via mitochondrial ROS to stimulate catabolism in C2C12 myotubes. *Am J Physiol Cell Physiol 302*(1), C195-C202.

Greish, K., Sawa, T., Fang, J., Akaike, T. & Maeda, H. SMA-doxorubicin, a new polymeric micellar drug for effective targeting to solid tumours. *J Controlled Release, 97*(2), 219-230.

Hale, J.P. & Lewis, I.J. (1994). Anthracyclines: cardiotoxicity and its prevention. *Arch Dis Child, 71*, 457-462.

Hole, P.S., Darley, R.L, & Tonks A. (2011). Do reactive oxygen species play a role in myeloid leukemias? *AM J Hematol 117*(22), 5816-5826.

Holloszy, J.O & Coyle, E.F. (1984). Adaptations of skeletal muscle to endurance exercise and their metabolic consequences. *J applied Phys 56*(4), 831-838.

Hortobagyi, G.N. (1997). Anthracyclines in the treatment of cancer. An overview. *Drugs, 54*(4), 1-7.

Hoydal, M.A., Wisloff, U., Kemi, O.J., Britton, S.L., Koch, L.G., Smith, G.L., & Ellingsen O. Nitric oxide synthase type-1 modulates cardiomyocyte contractility and calcium handling: association with low intrinsic aerobic capacity. *Eur J Cardiovasc Prev Rehab, 14*(2), 319-325.

Hrdina, R., Gersl, V, Klimtova, I & Simunek, T. (2000). Anthracycline-induced cardiotoxicity. *Acta Medica, 43*, 75-82.

Johnson, B.A. & Cheang, M.S. (1986). Comparison of Adriamycin uptake in chick embryo heart and liver cells and murine L5178Y lymphoblasts *in vitro*: Role of drug uptake in cardiotoxicity. *Cancer Res* 46*,* 218-223.

Jones, L.W. Peppercorn, J., Scott, J.M. & Battaglini, C. (2010). Exercise therapy in the management of solid tumors. *Curr Treat Options Oncol11,* 45-58.

Jones, R.L., Swanton, C. & Ewer, M.S. (2006). Anthracycline cardio-toxicity. *Expert Opin Drug Saf, 5,* 791-809.

Kavazis, A.N., Smuder, A.J., & Powers, S.K. (2010). Short-term exercise training protects against doxorubicin-induced cardiac mitochondrial damage independent of HSP72. *Am J Physiol Heart Circ Physiol, 299*, H1515-1524.

Keefe, D.M. & Bateman, E.H. (2012). Tumor control versus adverse events with targeted anticancer therapies. *Nat Rev Clin Oncol, 9*, 98-109.

Khakoo, A.Y, Liu, P.P., Force, T. & Lopez-Berestein, G. (2011). Cardiotoxicity due to cancer therapy. *Tex Heart Inst J, 38*(3), 253-256.

Kim, J.K., Pedram, A., Razandi, M. & Levin, E.R. (2005). Estrogen prevents cardiomyocyte apoptosis through inhibition of reactive oxygen species and differential regulation of P38 kinase isoforms. *J Bio Chem 281*, 6760-6767.

Kizek, R., Adam, V., & S. M. (2012). Anthracyclines and ellipticines as DNA-damaging anticancer drugs: recent advances. *J Pharm Thera, 133*, 26-39.

Koch, L.G. & Britton, S.L. (2001). Artificial selection for intrinsic aerobic endurance running capacity in rats. *Physiol Genomics*, *5* (1), 45-52.

Koch, L.G. & Britton, S.L. (2008). Aerobic metabolism underlies complexity and capacity. *J Physiol*, *586* (1), 83-95.

Koch, L.G. & Britton, S.L. (2008). Development of animal models to test the fundamental basis of gene-environment interactions. *Obesity*, *16* (3), S28-32.

Koch, L.G., Kemi, O.J., Qi, N. & Wisloff, U. (2011). Intrinsic aerobic capacity sets a divide for aging and longevity. *Circ Res109*, 1162-1172.

Koka S. & Kukreja R.C. (2010). Attenuation of doxorubicin-induced cardiotoxicity by tadalafil: a long acting phosphodiesterase-5 inhibitor. *Mol Cell Pharmacol, 2*(5), 173-178.

Kompare, M. & Rizzo, W.B. (2008). Mitochondrial fatty-acid oxidation disorders. *Semin Pediatr Neurol 15*, 140-149.

Korshunov, S.S., Skulachev, V.P. & Starkov, A.A. (1997). High protonic potential actuates a mechanism of production of reactive oxygen species in mitochondria. *FEBS letters 416,* 15-18.

Kristal, B., Park, B., & Yu, B.P. (1994). Antioxidants reduce peroxyl-mediated inhibition of mitochondrial transcription. *Free Rad Biol Med 16*, 653-660.

Lai, H.C, Yeh, Y.C., Wang, L.C. & Liu T.J. (2011). Propofol ameliorates doxorubicin-induced oxidative stress and cellular apoptosis in rat cardiomyoctyes. *J Taap 257* (3), 437-448.

Lang, K., L.M. Lines, D.W. Lee, J.R. Korn, C.C. Earle, & J. Menzin. (2009). Lifetime and treatment-phase costs associated with colorectal cancer: Evidence from SEER-Medicare Data. *Clinical and Gastroenterology and Hepatology 7* (2), 198-204.

L'Ecuyer, T.L., Sanjeev, s., Thomas, R., Novak, R. & Heide, R.V. (2006). DNA damage is an early event in doxorubicin-induced cardiac myocyte death. *Am J Physiol Heart Circ Physiol 291*, H1273-1280.

Lesnefsky, E.J., He, D., Moghaddas, S., & Hoppel, C.L. (2006). Reversal of mitochondrial defects before ischemia protects the aged heart. *FASEB J (20)*, 1543-1545.

Lemieux, H., Vasquez, E.J., Fujioka, H. & Hoppel, C.L. (2010). Decrease in mitochondrial function in rat cardiac permeabilized fibers correlates with the aging phenotype. *J Gerontol A Biol Sci Med Sci65A(*11), 1157-1164.

Lessard, S.J., Rivas, D.A., Chen, Z., Koch, L.G., Britton, S.L. & Hawley, J.A. (2009). Impaired skeletal muscle B-adrenergic activation and lipolysis are associated with whole-body insulin resistance in rats bred for low intrinsic exercise capacity. *Endo 150* (11), 4883-4891.

Leverve, X., Batandier, C. & Fontaine E. (2007). Choosing the right substrate. *Novartis Found Symp 280*, 108-121.

Ludke, A., Sharm, A.K., Bagchi, A.K. & Singal, P.K. (2011). Subcellular basis of vitamin C protection against doxorubicin-induced changes in rat cardiomyocytes. *Mol Cell Biochem (360)*, 215-224.

Martins, R.A., Minari, A.L., Chaves, M.D., Ribeiro, D.A. (2012). Exercise preconditioning modulates genotoxicity induced by doxorubicin in multiple organs of rats. *Cell Biochem Funct.*

McCormack, J.G., Stanley, W.C., & Wolff, A.A. (1998). Ranolazine: a novel metabolic modulator for the treatment of angina. *Gen Pharmac 30*(5), 639-645.

Moinuddin, I.K., Collins, E.G., Kramer, H.J. & Leehey, D.J. (2012). Exercise in the management of obesity. *J Obes Weigh los Ther 2*(2), 117-139.

Moghaddas, S., Stoll, M.S., Minkler, P.E., Salomon, R.G. & Hoppel C.L. (2002). Preservation of cardiolipin content during aging in rat heart interfibrillar mitochondria. *J Gerontol Biol Sci, 57*, B22-28.

Mokni, M., Hamlaoui-Guesmi, S. & Aouani, E. (2012). Grape seed and skin extract protects against acute chemotherapy toxicity induced by doxorubicin in rat heart. *Cardiovasc Toxicol 12*, 158-165.

Muller, I., Niethammer, D., & Bruchelt G. (1998). Anthracycline-derived chemotherapeutics in apoptosis and free radical cytotoxicity (Review). *Inter J MolMed 1*(2), 491-495.

Murry, C.E. & Lee, R.T. (2009). Turnover after the fallout. *Science 324*, 47-8.

Myers, C.E., McGuire, W.P., Liss, R.H. & Ifrim I. (1977). Adriamycin: the role of lipid peroxidation in cardiac toxicity and tumor response. *Science, 197,* 165-167.

Myers, J. Prakash, M., Froelicher, V. & Atwood, J.E. (2002). Exercise capacity and mortality among men referred for exercise testing *N Engl J Med 346,* 793-801.

National Heart Lung and Blood Institute: National Institutes of Health. *NHLBI Factbook, fiscal year 2010.* Washington (DC): US Department of Health and Human Services. (2012).

Nediani, C. Raimondi, L. & Cerbai E. (2011). Nitric oxide/reactive oxygen species generation and nitroso/redox imbalance in heart failure: from molecular mechanism to therapeutic implications. *Antioxid Redox Sign 14*(2), 289-331.

Nicholson G.L. & Conkin, K.A. (2008). Reversing mitochondrial dysfunction, fatigue and the adverse effects of chemotherapy of metastatic disease by molecular replacement therapy. *Clin Exp Metas*, *25*(2), 161-169.

Noland, R.C., Thyfault, J.P., & Henes, S.T. (2007). Artificial selection for high capacity endurance running is protective against high fat diet-induced insulin resistance. *Am J Physiol Endocrinol Metab 293,* E31-41.

Oliveira, A.M., Nuno, M., Bernado, T. & Sardao, V. (2011). Mitochondria as a biosensor for drug-induced toxicity – is it really relevant? Biosensors for health, environment and biosercurity, Pier Andrea Serra (Ed.), InTech.

Palpant, N.J. Szatkowski, M.L. and Metzger, J.M. (2009). Artificial selection for whole animal low intrinsic aerobic capacity co-segregates with hypoxia-induced cardiac pump failure. *Plos One 4*(7), 1-12.

Pereria, G.C., Silva, A.M., Diogo, C.V. & Oliveira, P.J. (2011). Drug-induced cardiac mitochondrial toxicity and protection: from doxorubicin to carvedilol. *Curr Pharm Des 17,* 2113-2129.

Quindry, J., French, J., Hamilton, K., Lee, Y., Mehta, J.L. and Powers, S. (2005). Exercise training provides cardioprotection against ischemia-reperfusion induced apoptosis in young and old animals. *Exp Geron 40*(5), 416-425.

Radi, R. Turren, J.F., Chang, L.Y. & Freeman, B.A. (1991). Detection of catalase in rat heart mitochondria. *J Biol Chem 266*, 22028-22034.

Rajagopalan , S., Politi, P.M., & Sinha, B.K. (1988). Adriamycin-induced free radical formation in the perfused rat heart: Implications for cardiotoxicity. *Cancer Res 48*, 4766-4769.

Rivas D.A., Lessard, S.J., Saito, M., Koch, L.G., Britton, S.L, & Hawley J.A. (2011). Low intrinsic running capacity is associated with reduced skeletal muscle substrate oxidation and lower mitochondrial content in white skeletal muscle. *Am J Physiol Regul Integr Comp Physiol 300*(4), R835-843.

Rognmo, O. Hetland, E., Hoff, J. & Slordahl, S.A. (2004). High intensity aerobic interval exercise is superior to moderate intensity exercise for increasing aerobic capacity in patients with coronary artery disease. *Eur J Cardiovasc Prev Rehabil 11*(3), 216-222.

Scandalios, J.G. (2002). Oxidative stress response – what have genome-scale studies taught us? *Gen Bio 3*(7), 1019..1-1019.6.

Schuh, R.A., Jackson, K.C., Khairallah, R.J., Ward, C.W. & Spangenburg, E.E. (2011). Measuring mitochondrial respiration in intact single muscle fibers. *Am J Physiol Regul Integr Comp Physiol 302*, R712-719.

Schwartz, E.R., Pollick, C., Dow, J., Patterson, M., Birnbaum, Y. & Kloner, R.A. (1998). A small animal model of non-ischemic cardiomyopathy and its evaluation by transthoracic echocardiography. *Cardio Res 39*, 216-223.

Scialdone, L. (2012). Overview of supportive care in patients receiving chemotherapy: antiemetics, pain management, anemia, and neutropenia. *J Pharm Pract, 00*(0), 1-13.

Shah, S.V. (2004). Oxidants and iron in chronic kidney disease. *Kidney Inter 66,* S50-S55.

Shan, K., Lincoff, A.M., & Young, J.B. (1996). Anthracycline-induced cardiotoxicity. *Ann Intern Med, 125,* 47-58.

Siegel, R., Desantis, C., & Virgo, K., Stein, K. & Mariotto, A. (2012). Cancer treatment and survivorship statistics, 2012. *CA Cancer J Clin.*

Siegel, R., Naishadham, D., & Jemal, A. (2012). Cancer statistics, 2012. *CA Cancer J Clin, 62*(1), 10-29.

Silber, J.H., Jakacki, R.I., Larsen, R.L., Goldwein, J.W., & Barber, G. (1993). Increased risk of cardiac dysfunction after anthracyclines in girls. *Med Ped Onc 21*, 477-479.

Simunek, T., Sterba, M., Popelova, O., Adamcova, M., Hrdina, R. & Gersi, V. (2009). Anthracycline-induced cardiotoxicity: overview of studies examining the roles of oxidative stress and free cellular iron. *Pharm Rep, 61,* 154-171.

Singal, P.K., Iliskovic, N., Li, T. & Kumar, D. (1997). Adriamycin cardiomyopathy: pathophysiology and prevention. *FASEB J, 11*(12), 931-936.

Singal, P.K. & Iliskovic, N. (1998). Doxorubicin-induced cardiomyopathy. *N Engl J Med 339,* 900-905.

Stanley, W.C., Recchhia, F.A & Lopaschuk, G.D. (2004). Myocardial substrate metabolism in the normal and failing heart. *Physiol Rev, 85*(3), 1093-1129.

Stevenson, C.S., Koch, L.G. & Britton, S.L. (2006). Aerobic capacity, oxidant stress, and chronic obstructive pulmonary disease – a new take on an old hypothesis. *Pharm Ther110*, 71-82.

Swain, S.M., Whaley, F.S., Ewer, M.S. (2003). Congestive heart failure in patients treated with doxorubicin. *Cancer, 97*(11), 2869-2879.

Tang, Z., Iqbal, M., Cawthon, D., & Bottje, W.G. (2002). Heart and breast muscle mitochondrial dysfunction in pulmonary hypertension syndrome in broilers (*Gallus domesticus)*. *Comp Biochem Physiol 132,*527-540.

Tokarska-Schlattner, M., Zaugg, M. & Schlattner U. (2006). New insights into doxorubicin-induced cardiotoxicity: the critical role of cellular energetics. *J Mol Cell Cardiol 41*, 389-405.

Trachtenberg, B.H., Landy, D.C., & Lipshultz, S.E. (2011). Anthracycline-associated cardiotoxicity in survivors of childhood cancer. *Pediatr Cardiol 32,* 342-353.

Tweedie, C., Romestaing, C., Burelle, Y., Britton, S.L., Koch, L.G. & Hepple, R.T. (2011). Lower oxidative DNA damage despite greater ROS production in muscles from rats selectively bred for high running capacity. *AJP – Regu Physiol 300*(3), R544-R553.

Wallace, K.B. (2003). Doxorubicin-induced cardiac mitochondrionopathy. *Pharm & Toxic 93,* 105-115.

Walsh, B., Hooks, R.B., Hornyak, J.E., Koch, L.G. & Britton, S.L. (2006). Enhanced mitochondrial sensitivity to creatine in rats bred for high aerobic capacity. *J Appl Physiol100,* 1765-1769.

Wang, S., Konorev, E.A., Kotamraju, S., Joseph, J., Kalivendi, S. & Kalyanaraman, B. (2004). Doxorubicin induces apoptosis in normal and tumor cells via distinctly different mechanisms. *J Biol Chem 279*, 25535-25543.

Wapstra, F.H., van Goor, H., de Jong, P.E., Navis, G. & de Zeeuw, D. (1999). Dose of doxorubicin determines severity of renal damage and responsiveness to ACE-inhibition in experimental nephrosis. *J Pharm & Toxic Meth 41*, 69-73.

Waters, R.P., Renner, K.J., Pringle, R.B., Summer, C.H., Koch, L.G. & Swallow, J.G. (2008). Selection for aerobic capcity affects corticosterone monoamines and wheel-running activity. *Phys & Behav 93,* 1044-54.

Williamson, J.R. (1979) Mitochondrial function in the heart. *Annu Rev Physiol 41*, 485-506.

Wisloff, U., Najjar, S.M., Ellingsen, O., Koch, L.G., & Britton, S.L. (2005). Cardiovascular risk factors emerge after artificial selection for low aerobic capacity. *Science 307*(5708), 418-420.

Wojnowski, L., Kulle, B., Schirmer, M., Brockmuller, J. & Hasenfuss, G. (2005). NAD(P)H oxidase and multidrug resistance protein genetic polymorphisms are associated with doxorubicin-induced cardiotoxicity. *Circ 112*, 3754-3762.

Wondergem, J., Stephens, L.C. & Frederick R.S. (1991). Effect of adriamycin combined with whole body hyperthermia on tumor and normal tissues. *Cancer Res (51)*, 3559-3567.

Wonders, K.Y., Hydock, D.S., Schneider, C.M. & Hayward, R. (2008). Acute exercise protects against doxorubicin cardiotoxicity. *Integr Cancer Ther 7,* 147-154.

Wouters, K.A., Kremer, L.C., Miller, T.L., & Herman, E.H. (2005). Protecting against anthracyclines-induced myocardial damage: a review of the most promising strategies. *Br J Haematol, 131,* 561-578.

Von Hoff, D.D., Layard, M.W., Basa, P, Muggia, F.M. (1979). Risk factors for doxorubicin-induced congestive heart failure. *Ann Int Med 91,* 710-717.

Yan, Y., Liu, J., Wei, C., & Cheng, H. (2008). Bidirectional regulation fo Ca2+ sparks by mitochondria-derived reactive oxygen species in cardiac myocytes. *Cardiovasc Res (77)*, 432-441.

Yen, H.C., Oberley, T.D., Vichitbandha, S., Ho, Y.S., & St Clair, D.K. (1996). The protective role of manganese superoxide dismutase against adriamycin-induced acute cardiac toxicity in transgenic mice. *J Clin Invest 98*, 1253-1260.

Zhou, Z. & Kang, Y.J. (2000) Cellular and subcellular localization of catalase in the heart of transgenic mice. *J Histochem Cytochem 48(5)*, 585-594.

APPENDIX I. Institutional Animal Care And Use Committee Approval

East Carolina University

Animal Care and
Use Commitee
212 Ed Warren Life
Sciences Building
East Carolina University
Greenville, NC 27834

252-744-2436 office
252-744-2355 fax

April 25, 2011

Robert Lust, Ph.D.
Department of Physiology
Brody 6N-98
ECU Brody School of Medicine

Dear Dr. Lust:

Your Animal Use Protocol entitled, "Cardiovascular Consequences of Artificial Selection Based on Aerobic Running Capacity" (AUP #Q250a) was reviewed by this institution's Animal Care and Use Committee on 4/25/11. The following action was taken by the Committee:

"Approved as submitted"

A copy is enclosed for your laboratory files. Please be reminded that all animal procedures must be conducted as described in the approved Animal Use Protocol. Modifications of these procedures cannot be performed without prior approval of the ACUC. The Animal Welfare Act and Public Health Service Guidelines require the ACUC to suspend activities not in accordance with approved procedures and report such activities to the responsible University Official (Vice Chancellor for Health Sciences or Vice Chancellor for Academic Affairs) and appropriate federal Agencies.

Sincerely yours,

Scott E. Gordon, Ph.D.
Chairman, Animal Care and Use Committee

SEG/jd

enclosure

APPENDIX II. Institutional Approval of Safety Protocol for using Doxorubicin

APPENDIX 1 - HAZARDOUS AGENTS			
Principal Investigator: Bob Lust	Campus Phone:744-2761		Home Phone:756-3939
IACUC Protocol Number:Q250	Department: Physiology		E-Mail:lustr@ecu.edu
Secondary Contact: Laura Frye Department: Physiology	Campus Phone:744-2762	Home Phone:	E-Mail: fryel@ecu.edu
Chemical Agents Used: doxorubicin (adriamycin)		Radioisotopes Used: none	
Biohazardous Agents Used:		Animal Biosafety Level:1	Infectious to humans? No
PERSONAL PROTECTIVE EQUIPMENT REQUIRED:			
Route of Excretion: urine/feces; animal bedding to be considered contaminated for 48 hours after injection			
Precautions for Handling Live or Dead Animals: Wear standard personal protective equipment			
Animal Disposal: All materials will be discarded in biohazard bags and incinerated through ECU Hazardous Waste Management			
Bedding / Waste Disposal: All materials will be discarded in biohazard bags with a cancer hazard sticker and incinerated through ECU Hazardous Waste Management. After 48 hours after injection, bedding will be bagged and disposed of as municipal waste.			
Cage Decontamination: Normal cage washing will be sufficient			
Additional Precautions to Protect Personnel, Adjacent Research Projects including Animals and the Environment:			
Initial Approval Safety/Subject Matter Expert Signature & Date Kelly E. Shook 12/27/11			

1

APPENDIX III. Safety Protocol for using Doxorubicin

Laboratory Safety Plan for Doxorubicin Injection

*Process	Doxorubicin Injection
*Hazardous Chemical/ Chemical Class	Doxorubicin (Adriamycin) Possible carcinogen; target organs: reproductive system, heart and bone marrow
*Hazardous Equipment	Syringe
*Potential Hazards	Harmful if inhaled, ingested, absorbed through skin and eyes, accidentally injected. Poisonous vapors can increase in a fire. Potential carcinogen and mutagen; chronic exposure can lead to damage to heart, bone marrow and reproductive organs.
*Personal Protective Equipment	Closed front lab coat, closed toe shoes, nitrile gloves (double gloving is recommended), safety glasses/goggles
*Engineering and Ventilation Controls	All preparation and dilutions of the chemical will be done in certified chemical fume hood in Brody 3S-08. Animal injections will be done in certified chemcial fume hood in Brody GW-27. The floor of the hood will be covered with plastic backed paper liner. All extraneous equipment will be removed from the hood before work begins. All equipment required for preparing the solutions for injections and for filling syringes will be placed in the hood prior to beginning work. Tubes and vials containing these materials can only be removed from fume hood if tightly capped and the exterior wet wiped.
Designated Use Area for Carcinogens, Reproductive Toxins or Acute Toxins	Animal injections will take place in Brody GW27 chemical fume hood. Designated areas of use (certified chemical fume hood) will be decontaminated after use. The chemical will be stored in Brody 3S-08 in a separate container keeping it out of contact of other substances. It will be in a secondary container labeled with a chemotherapy hazard sticker and there will be absorbent material lining the secondary container. Final dilutions will be transferred to GW-27in secondary containment lined with plastic backed absorbent paper when moved for administration. Freight elevator or stairs will be used for transport.
Special Use Procedures	Drug delivery will be accomplished in a closed loop system. Syringes used for delivery will be sized large enough so that they are not full when the entire drug dose is present. Never re-cap syringes. Syringes will be disposed at the end of administration in a sharps disposal container labeled with the cancer hazard symbol.
Special Handling and Storage Requirements	Stock and prepared dilutions will be securely stored in Brody 3S-08. Containers will be segregated from other chemicals in secondary containment lined with plastic backed absorbent paper. The outside of the secondary container will have a chemotherapy hazard sticker attached. Keep tightly closed. Material will be placed in a red biohazard bag and labeled with a chemotherapy hazard sticker. A sharps disposal container, labeled with a chemotherapy hazard sticker will be used for empty syringe disposal after injection.
*Spill and Accident Procedures	Spills located in the fume hood will be cleaned by individuals trained to do so and wearing the standard protective equipment (gloves, labcoat, closed toe shoes, safety glasses/goggles). Wearing protective equipment, the liquid will be wiped with absorbent gauze pads and the spill area cleaned 3 times with soap and water. Any broken glass fragments will be collected with a scoop and brush, and placed in the sharps container labeled with the carcinogen hazard symbol. All clean-up material will be disposed through the ECU hazardous waste disposal system. If a spill takes place outside of a hood, call EH&S at 328-6166 and evacuate the area.
*Waste Minimization Plan	Smallest quantity required will be purchased
*Hazardous Waste Disposal	Syringes will be disposed at the end of administration in a sharps disposal container labeled with the carcinogen hazard symbol. Empty drug vials will be labeled with carcinogen hazard symbol and bagged in a hazardous waste plastic bag, and picked up through the hazardous waste disposal. Gloves and other items containing trace residues will be placed in a red biohazard bag with the carcinogen label affixed for disposal through the medical waste disposal system.
Decontamination Procedures	The hood will be decontaminated if there is an incident that would result in hood contaminated. This will be accomplished by removing the paper liner and wiping the hood interior surfaces with 70% alcohol from the top to bottom the back to front.
Animal Care Precautions	Animal care staff will wear nitrile gloves, isolation gown, closed toed shoes while handling bedding and other animal wastes. Animal waste formed during the 48 hours after chemotherapy injection needs to be handled separately and put into red biohazard bags and additionally labeled with chemotherapy hazard sticker. **The PI doing the chemotherapy injection will alert Dale Aycock, or covering supervisor in his absence, of when the injection of chemotherapy is given so animal care personnel can be informed of a change in hazard level.** Any animal carcasses will be placed in red biohazard bags, labeled with chemotherapy hazard sticker and placed in cooler for disposal.
*Chemical Procurement	Smallest quantity required will be purchased
*Revision Date	Insert December, 2011 Lab Room 3S-08

Kelly E. Shook
12/22/11

2